HUMAN GENE THERAPY 19:384–390 (April 2008)

DOI: 10.1089/hum.2007.167

Brief Report

Noninvasive *In Vivo* Delivery of Transgene via Adeno-Associated Virus into Supporting Cells of the Neonatal Mouse Cochlea

TAKASHI IIZUKA,[1] SHO KANZAKI,[2] HIDEKI MOCHIZUKI,[3] AYAKO INOSHITA,[1] YUYA NARUI,[1] MASAYUKI FURUKAWA,[1] TAKESHI KUSUNOKI,[1] MAKOTO SAJI,[4] KAORU OGAWA,[2] and KATSUHISA IKEDA[1]

ABSTRACT

There are a number of genetic diseases that affect the cochlea early in life, which require normal gene transfer in the early developmental stage to prevent deafness. The delivery of adenovirus (AdV) and adeno-associated virus (AAV) was investigated to elucidate the efficiency and cellular specificity of transgene expression in the neonatal mouse cochlea. The extent of AdV transfection is comparable to that obtained with adult mice. AAV-directed gene transfer after injection into the scala media through a cochleostomy showed transgene expression in the supporting cells, inner hair cells (IHCs), and lateral wall with resulting hearing loss. On the other hand, gene expression was observed in Deiters cells, IHCs, and lateral wall without hearing loss after the application of AAV into the scala tympani through the round window. These findings indicate that injection of AAV into the scala tympani of the neonatal mouse cochlea therefore has the potential to efficiently and noninvasively introduce transgenes to the cochlear supporting cells, and this modality is thus considered to be a promising strategy to prevent hereditary prelingual deafness.

INTRODUCTION

SEVERAL TYPES OF HEREDITARY DEAFNESS in humans have been matched with homologous mouse models (Eisen and Ryugo, 2007). Mice present an ideal model for inner ear gene therapy because their genome is being rapidly sequenced and their generation time is relatively short. To achieve effective gene therapy in hereditary deafness, it may be required to transfer corrective genes into the defective cochlear cells of neonatal mice. However, the small size of the neonatal mouse inner ear poses a particular challenge for performing surgical procedures.

Transgene expression has been successfully demonstrated in the mammalian inner ear, using various viral vectors including adenoviral (AdV) vectors (Raphael *et al.*, 1996), adeno-associated viral (AAV) vectors (Lalwani *et al.*,1996), herpes simplex viral vectors (Derby *et al.*, 1999), lentiviral vectors (Han *et al.*, 1999), and Sendai viral vectors (Kanzaki *et al.*, 2007). In this study, we tested AAV vectors and AdV vectors because AAVs are free of genotoxicity and present no evidence of pathogenicity in humans, and AdVs have high transfection efficiency in many tissues and cell types. In previous studies, the three main routes of delivery of viral vectors into the cochlea of the adult mouse, namely, the scala media approach, the semicircular canal approach, and the round window (RW) approach, have been reported (Kawamoto *et al.*, 2001; Suzuki *et al.*, 2003). The semicircular canal method was not used in this study because of its poor transduction of genes.

The present study assessed how to inject a gene into the neonatal mouse cochlea on postnatal day 0 (P0); the results indicate that this modality is a promising therapeutic strategy to prevent prelingual deafness.

[1]Department of Otorhinolaryngology, Juntendo University School of Medicine, Tokyo 113-8421, Japan.
[2]Department of Otolaryngology, Keio University, Tokyo 160-0016, Japan.
[3]Department of Neurology, Juntendo University School of Medicine, Tokyo 113-8421, Japan.
[4]Department of Physiology, School of Allied Health Sciences, Kitasato University, Sagamihara 228-8555, Japan.

MATERIALS AND METHODS

Animals

Twenty healthy C57BL/6 mouse pups, irrespective of gender, were used on P0 (within 24 hr of birth). All experimental protocols were approved by the Institutional Animal Care and Use Committee at Juntendo University (Tokyo, Japan), and were conducted in accordance with the U.S. National Institutes of Health *Guide for the Care and Use of Laboratory Animals*.

Adenoviral and adeno-associated viral vectors

A replication-deficient adenoviral vector (human AdV, serotype 5) was used to encode the green fluorescent protein (GFP) driven by the cytomegalovirus (CMV) promoter. The virus was designated Ad5.CMV-GFP (3×10^{11} plaque-forming units [PFU]/ml). The E1 and E3 regions were deleted. Vectors were purchased from Primmune KK (Osaka, Japan). Viral suspensions in 10 m*M* Tris-HCl (pH 7.5), 1 m*M* $MgCl_2$, and 10% glycerol were kept at –80°C until thawed for use.

The plasmid DNA pAAV-MCS (CMV promoter; Stratagene, La Jolla, CA) carrying the GFP gene was constructed as reported previously (Yamada *et al.*, 2004). The plasmid DNA pAAV-GFP was cotransfected with plasmids pHelper and Pack2/1 into HEK-293 cells, using the standard calcium phosphate method (Sambrook and Russell, 2001). After 48 hr, cells were harvested and crude recombinant AAV (rAAV) vector (serotype 1) solutions were obtained by repeated freeze–thaw cycles. After ammonium sulfate precipitation, the viral particles were dissolved in phosphate-buffered saline (PBS) and applied to an OptiSeal centrifugation tube (Beckman Coulter, Fullerton, CA). After overlaying OptiPrep solution (Axis-Shield PoC, Oslo, Norway), the tube was processed with a Gradient Master (BioComp Instruments, Fredericton, NB, Canada) to prepare a gradient layer of OptiPrep. The tube was then ultracentrifuged at 13,000 rpm for 18.5 hr. The fractions containing high-titer rAAV vectors were collected and used for injection into animals. The number of rAAV genome copies was semiquantified by polymerase chain reaction (PCR) within the CMV promoter region using primers 5′-GACGTCAATAATGACGTATG-3′ and 5′-GGTAATAGCGATGACTAATACG-3′. The final titer was 1.4×10^{13} viral particles (VP)/ml.

Surgical procedures

Glass capillaries (Drummond Scientific, Broomall, PA) were drawn with a PB-7 pipette puller (Narishige, Tokyo, Japan) to achieve an approximately 10-μm outer tip diameter. A polyethylene tube (outer diameter, 1.7 mm; Atom Medical, Saitama, Japan) was connected to the glass micropipette.

For injection into the scala media via a cochleostomy, C57BL/6 mice were anesthetized with ketamine (100 mg/kg) and xylazine (4 mg/kg) by intraperitoneal injection. A left postauricular incision was made and the otic bulla was exposed, and opened to expose the cochlea. A cochleostomy was made at the cochlear lateral wall of a basal turn just beneath the stapedial artery with the glass micropipette, using a micromanipulator. The bony lateral wall of the cochlea on P0 is so soft that it can be easily penetrated by the glass micropipette. The injection volume of the viral vector was regulated at approximately 0.02 μl/min for 10 min, using a syringe connected to the polyethylene tube. To allow the vector to spread throughout and stabilize in the inner ear, the glass micropipette was left in place for 1 min after the injection. The hole was plugged and the opening in the tympanic bulla was sealed with connective tissue. The total surgical period was approximately 20 min.

For injection into the scala tympani after anesthesia, the otic bulla was opened to expose the RW. Next, the glass micropipette was inserted into the RW (Fig. 1), and the vectors were injected in the same manner as in the scala media approach. Because the hole in the RW membrane was extremely small, leakage of perilymph was found to be nominal after re-

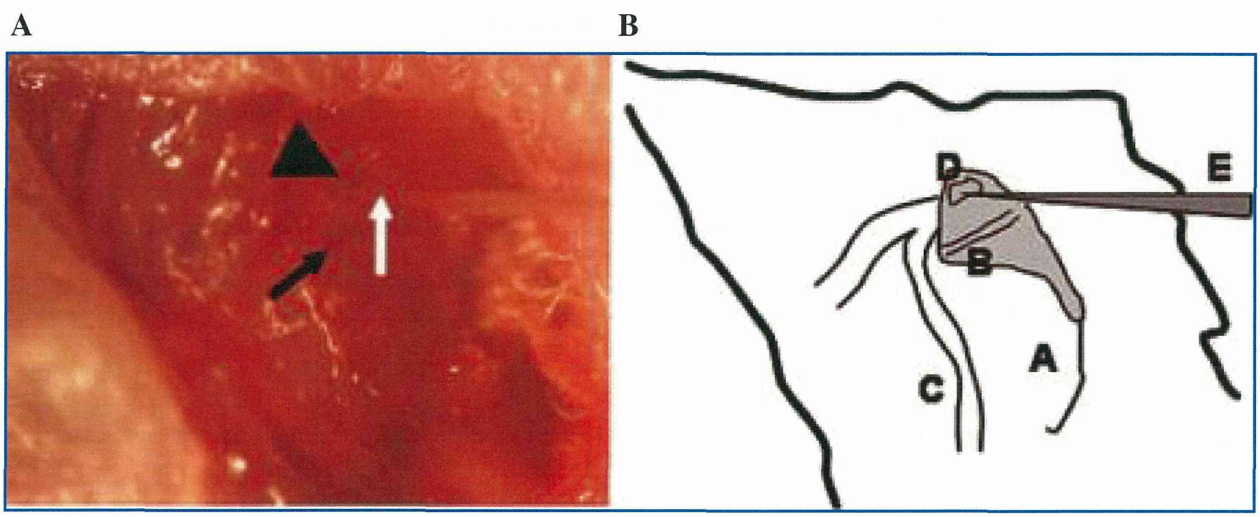

FIG. 1. Surgical procedure for microinjection into the neonatal mouse cochlea. The otic bulla was exposed after a left postauricular incision. The otic bulla is transparent. After opening the otic bulla, a round window (arrowhead) and the stapedial artery (solid arrow) are seen. Viral vectors were injected into the scala tympani with a glass micropipette (open arrow) inserted into the RW membrane. A, tympanic bulla; B, stapedial artery; C, facial nerve; D, round window; E, glass micropipette.

moving the micropipette. It took approximately 20 min to complete the surgical procedure. After the surgery, the mice were kept in another cage until they awoke from anesthesia.

Measurements of auditory brainstem response

To determine the surgical effects on auditory function, the auditory brainstem response (ABR) were assessed 14 days postoperatively. Hearing thresholds were determined in both ears: the injected side (left) and the contralateral noninjected control side (right). ABR measurements were performed as previously reported (Kanzaki *et al.*, 2007). Thresholds were determined for frequencies of 4, 8, 12, 16, and 20 kHz from a set of responses at various intensities with 5-dB intervals and electrical signals were averaged at 512 repetitions. If the hearing threshold was over 95 dB, then it was determined to be 100 dB.

Sample preparation, histology, and immunohistochemical analysis

On day 14 after injection, the mice were deeply anesthetized and perfused intracardially with PBS, followed by 4% paraformaldehyde in phosphate buffer. The cochleae were excised and then tissue specimens were fixed in 4% paraformaldehyde for 2 hr and decalcified in 0.12 *M* EDTA for 7 days at room temperature. For frozen sections, specimens were cryoprotected in 30% sucrose in PBS overnight at 4°C, and then were embedded, frozen, and sectioned at 10 μm. For immunofluorescence, sections were incubated with 50% Block Ace (AbD Serotec/MorphoSys, Martinsried, Germany) in PBS–0.3% Triton X-100 for 60 min and then they were incubated overnight at 4°C with goat polyclonal anti-GFP antibodies (diluted 1:200 in PBS; Santa Cruz Biotechnology, Santa Cruz, CA). The next day, tissue specimens were rinsed with PBS, incubated for 60 min with rabbit anti-goat IgG antibodies conjugated with Alexa Fluor 488 (diluted 1:500; Invitrogen Molecular Probes, Eugene, OR), and rinsed with PBS. Subsequently, all specimens were incubated with rhodamine phalloidin (diluted 1:100; Invitrogen Molecular Probes) for 30 min and then were mounted in VECTASHIELD antifade mounting medium with 4′,6-diamidino-2-phenylindole (DAPI; Vector Laboratories, Burlingame, CA).

Images of sections were captured with a Zeiss Axioplan 2 microscope (Carl Zeiss, Oberkochen, Germany), using an AxioCam HRc charge-coupled device (CCD) camera and the AxioVision release 4.5 software program.

Data analysis

The KaleidaGraph statistical software program (Synergy Software, Reading, PA) was used for the statistical analysis of the ABR data.

RESULTS

All of the animals recovered uneventfully from surgery and survived until ABR measurements were performed. No signs of vestibular disturbance, such as circling behavior or head tilting, were observed.

After the injection of AdV vectors into the scala media (n = 3), GFP-positive cells were present mainly in the supporting cells (Fig. 2A), mesothelial cells of the scala tympani and scala vestibuli, and cells of Reissner's membrane. Injection of AdV through the RW (n = 5) induced the expression of GFP only in the mesothelial cells lining the perilymphatic spaces (Fig. 2B). No GFP-positive cells were found in either the organ of Corti or the lateral wall. GFP expression was identified in various cochlear cells (Fig. 2C), predominantly in both the inner hair cells and the supporting cells of the organ of Corti after AAV injection into the scala media (n = 6), and the loss of hair cells, as noted in a previous report (Ishimoto *et al.*, 2002), was not observed in these mice (Fig. 2D). Application of AAV to the scala tympani across the RW (n = 6) showed that GFP-positive cells were found mainly in the supporting cells (Fig. 2E), and loss of hair cells was not (Fig. 2F). These results are summarized in Table 1. An examination of the contralateral (right) ears of AAV injected mice revealed a normal appearance with no pathological hair cell loss, and no GFP-positive cells were seen (Fig. 2G and H).

Before killing the mice on P14, ABR thresholds were assessed in both ears, on both the injected side and contralateral side. In the groups injected with AAV (Fig. 3A) or AdV vectors (Fig. 3B) by the scala tympani approach through the RW, the ABR thresholds did not differ significantly from those of contralateral noninjected control sides at any frequency tested. On the other hand, a significant threshold shift at each frequency was seen in the group injected with either AAV (Fig. 3C) or AdV vectors (Fig. 3D) by the scala media approach via cochleostomy, in comparison with those on the contralateral control sides.

DISCUSSION

To our knowledge this is the first report demonstrating successful gene delivery to the neonatal mouse cochlea *in vivo*. It is ideal to transfer a normal gene noninvasively to a hereditary deafness mouse model at an early time after birth, before differentiation of the cochlear sensory structures. The procedure of gene delivery to the animal models must yield efficient gene transduction without hearing loss.

Excellent gene expression without hearing loss was obtained by selecting both the appropriate application route (the

FIG. 2. Sagittal cryosections of the mouse cochlea. GFP-expressing cells (green) are seen by fluorescence microscopy in cochlear sagittal cryosections of P14 mice that had been injected on P0. Rhodamine phalloidin antibody was used as a marker for hair cells (red). (**A**) Cochlear section after exposure to AdV by scala media injection. Transduced Deiters cells and outer pillar cells (arrows) expressed GFP. (**B**) After exposure to AdV by scala tympani injection. Only mesothelial cells of the perilymph expressed GFP. GFP were absent in the organ of Corti. (**C** and **D**) Cochlear section after exposure to AAV by scala media injection. (**C**) Transduced supporting cells (Deiters cells, Hensen cells, and Claudius cells; arrowheads) expressed GFP. (**D**) No loss of hair cells was observed with the nuclear label DAPI (blue). (**E** and **F**) After exposure to AAV by scala tympani injection, transduced Deiters cells (arrows) expressed GFP (**E**), and loss of hair cells was not observed (**F**). (**G** and **H**) Cochlear section of contralateral (right) ears after exposure to AAV by both scala media injection (**G**) and scala tympani injection (**H**) revealed a normal appearance with no pathological hair cell loss, and no GFP-positive cells were seen. Scale bar in (**A**) (for **A–H**): 100 μm.

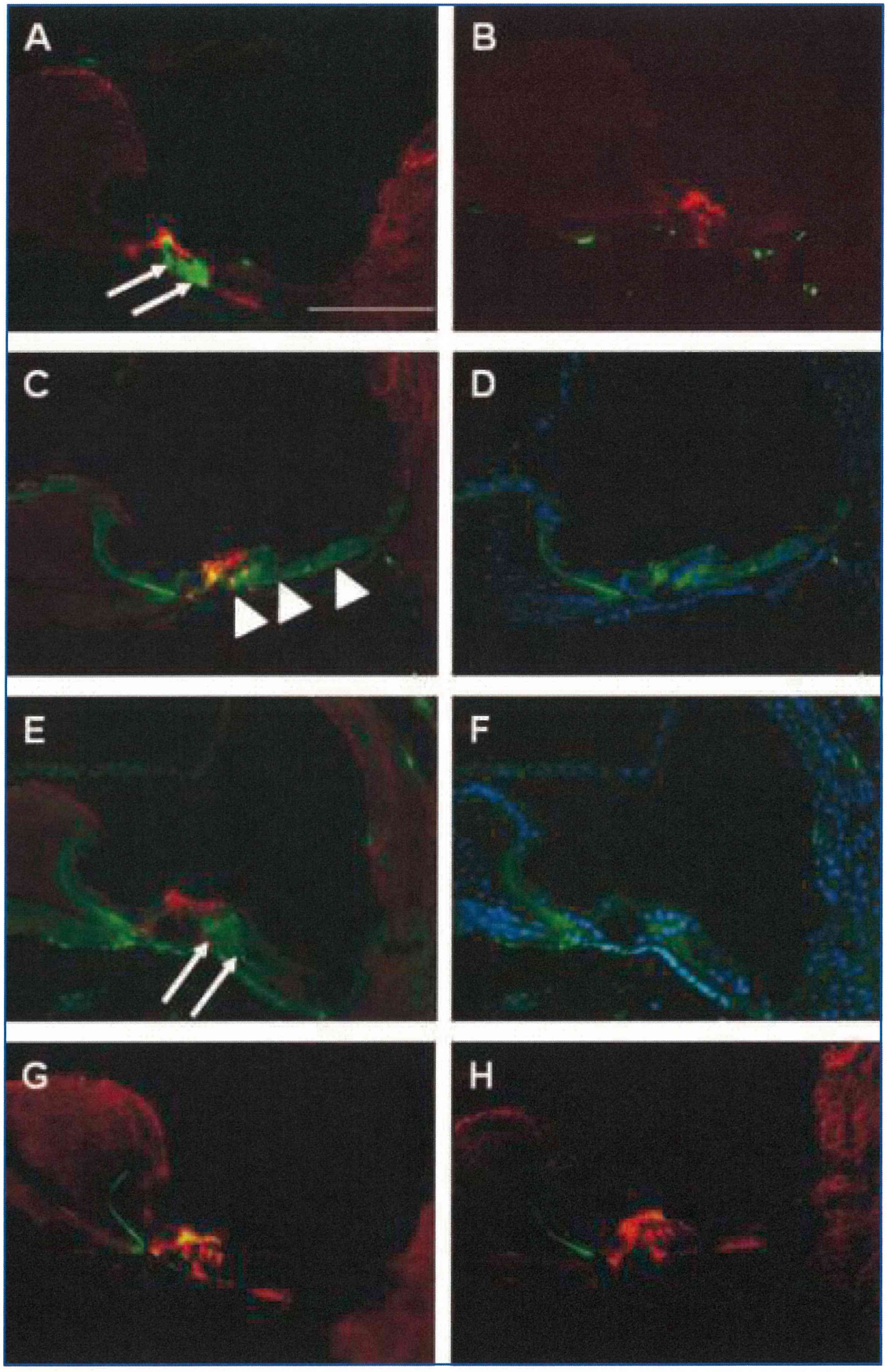

FIG. 2.

TABLE 1. EXPRESSION OF TRANSGENE IN MOUSE COCHLEAR CELLS

Vector	*Injection place*	*Total number*	*Inner hair cells*	*Outer hair cells*	*Pillar cells*	*Deiters cells*	*Hensen cells*	*Claudious cells*	*Inner sulcus cells*	*Outer sulcus cells*	*Stria vascularis*	*Spiral ganglion*	*Spiral ligament*	*Reissner's membrane*	*Spiral limbus*	*Mesothelial cells*
AAV	RW	$n = 6$	6	—	—	5	4	3	2	2	4	2	6	1	2	5
	Cochleostomy	$n = 6$	6	1	1	5	5	5	4	5	5	—	6	3	6	5
AdV	RW	$n = 5$	—	—	—	—	—	—	—	—	—	—	—	2	1	5
	Cochleostomy	$n = 3$	1	—	2	3	—	—	—	—	—	—	1	2	—	3

Abbreviations: AAV, adeno-associated virus; AdV, adenovirus; RW, round window.

[a]AAV or AdV was applied to the cochlea via the RW or cochleostomoy approach. Transgene expression the various cells of the inner ear was detected by the presence of green fluorescent protein.

[b]A dash (—) indicates no fluorescence in cells of the infected mouse cochlea.

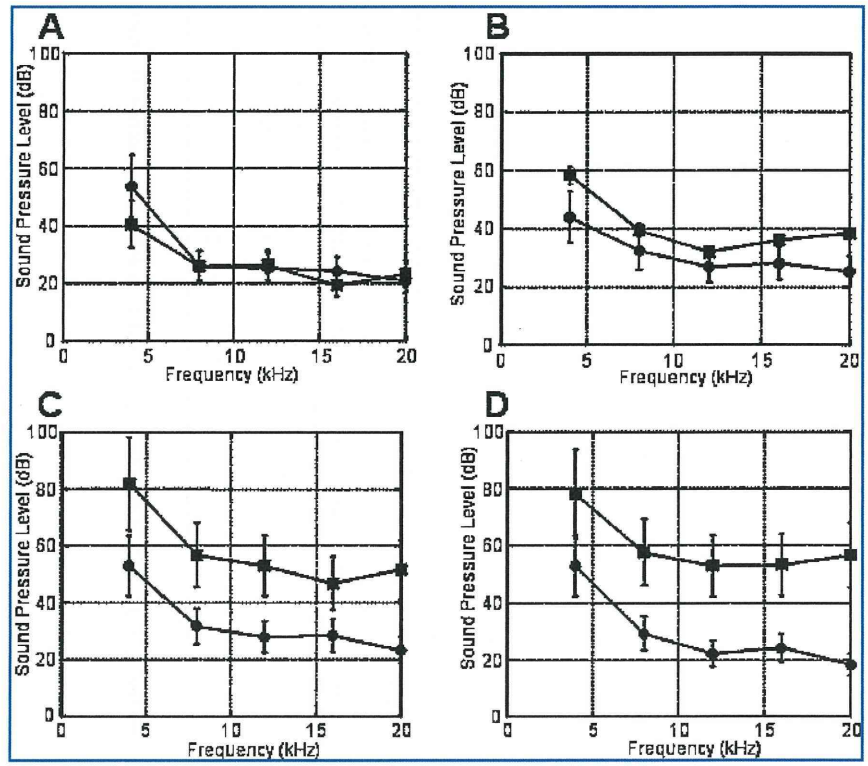

FIG. 3. ABR thresholds in mice after gene transfer. Threshold shifts at all frequencies were less than 15 dB in comparison with the contralateral side (*right*, solid circles) after the injection of AAV (**A**) or AdV (**B**) into the scala tympani (*left*, solid squares). On the other hand, injection of AAV (**C**) or AdV (**D**) into the scala media resulted in an elevation of ABR thresholds at all frequencies.

RW approach) and viral vector (AAV) for the neonatal mouse cochlea. The extent of AdV transfection was extremely limited in the mesenchymal cells, comparable to that obtained with adult mice; gene expression after AAV transfection by the RW approach was seen mainly in the cochlear supporting cells.

AAV serotype 1 was chosen on the basis of previously published reports indicating that AAV serotype 2 was unable to transduce hair cells or supporting cells of the cochlea either *in vivo* or *in vitro* (Kho *et al.*, 2000; Jero *et al.*, 2001a; Luebke *et al.*, 2001). There have been no reports demonstrating gene expression in supporting cells without hearing loss after injection into either the neonatal or adult mouse cochlea (Lalwani *et al.*, 1996, 1998; Jero *et al.*, 2001a; Luebke *et al.*, 2001; Duan *et al.*, 2002; Liu *et al.*, 2005, 2007).

When administering AdV in a cochlear organ culture, transgene expression was seen in most hair cells on P0 and in supporting cells on P3 to P5 (Kanzaki *et al.*, 2002). This study also demonstrates that AdV-mediated transgene expression was seen in both hair cells and supporting cells. On the other hand, transduction of P0 explants with AAV serotype 1 thus results in expression in the inner and outer hair cells, Hensen cells, and interdental cells (Stone *et al.*, 2005). In the present study, gene expression was also found mainly in supporting cells and inner hair cells on P0 *in vivo*, but not in supporting cells of the adult mouse as reported in previous studies. The difference in gene expression between adult and neonate may be explained in that supporting cells of the adult mouse do not have sialic acid on their surface as receptors for viral entry whereas those of the neonatal mouse do.

There are a number of genetic diseases that affect the cochlea early in life. *GJB2*, encoding gap junctional protein connexin26 (Cx26), which is expressed in supporting cells of the organ of Corti, is responsible for approximately half of all hereditary deafness cases (Kelsell *et al.*, 1997; Chang *et al.*, 2003). Animal models of both a conditional knockout of *Gjb2* (Cohen-Salmon *et al.*, 2002) and a dominant-negative *Gjb2* mutation (Kudo *et al.*, 2003) suggest that a critical but unknown function of the supporting cells is disturbed primarily by defective Cx26. Cx26 in the organ of Corti is extensively expressed in the mouse cochlea from birth (Frenz and Water, 2000; Zhang *et al.*, 2005). Furthermore, a dominant-negative *Gjb2* mutant mouse showed incomplete development of the cochlear supporting cells in our preliminary data. Thus, it is possible that the *Gjb2* mutation could be successfully treated by gene delivery to introduce the normal gene to the supporting cells of the neonatal cochlea.

In conclusion, this study has demonstrated excellent gene expression in supporting cells of the neonatal mouse cochlea, with good preservation of auditory function. It is therefore considered to be possible to repair hearing loss by applying the present method to the animal model of the *Gjb2* mutation, thereby suggesting the potential future effectiveness of such a modality for the development of gene-based therapies for humans.

ACKNOWLEDGMENTS

The authors thank Ms. J. Onoda, Mr. T. Yasuda, and Ms. T. Nihira for valuable technical assistance.

AUTHOR DISCLOSURE STATEMENT

No competing financial interests exist.

REFERENCES

CHANG, E.H., VAN CAMP, G., and SMITH, R.J. (2003). The role of connexins in human disease. Ear Hear. **24,** 314–323.

COHEN-SALMON, M., OTT, T., MICHEL, V., HARDELIN, J.P., PERFETTINI, I., EYBALIN, M., WU, T., MARCUS, D.C., WANGEMANN, P., WILLECKE, K., and PETIT, C. (2002). Target ablation of connexin26 in the inner ear epithelial gap junction network causes hearing impairment and cell death. Curr. Biol. **12,** 1106–1111.

DERBY, M.L., SENA-ESTEVES, M., BREAKEFIELD, X.O., and COREY, D.P. (1999). Gene transfer into the mammalian inner ear using HSV-1 and vaccine virus vectors. Hear. Res. **134,** 1–8.

DUAN, M.L., BORDET, T., MEZZINA, M., KAHN, A., and ULFENDAHL, M. (2002). Adenoviral and adeno-associated viral vector mediated gene transfer in the guinea pig cochlea. Neuroreport **13,** 1295–1299.

EISEN, M.D., and RYUGO, D.K. (2007). Hearing molecules: Contributions from genetic deafness. Cell. Mol. Life Sci. **64,** 566–580.

FRENZ, C.M., and WATER, T.R. (2000). Immunolocalization of connexin26 in the developing mouse cochlea. Brain Res. Rev. **32,** 172–180.

HAN, J.J., MHATRE, A.N., WAREING, M., PETTIS, R., ZUFFEREY, A.N., TRONO, D., and LALWANI, A.K. (1999). Transgene expression in the guinea pig cochlea mediated by the lentivirus-derived gene transfer vector. Hum. Gene Ther. **10,** 1867–1874.

ISHIMOTO, S., KAWAMOTO, K., KANZAKI, S., and RAPHAEL, Y. (2002). Gene transfer into supporting cells of organ of Corti. Hear. Res. **173,** 187–197.

JERO, J., MHATRE, A.N., TSENG, C.J., STERN, R.E., COLING, D.E., GOLDSTEIN, J.A., HONG, K., ZHENG, W.W., HOQUE, A.T.M.S., and LALWANI, A.K. (2001a). Cochlear gene delivery through an intact round window membrane in mouse. Hum. Gene Ther. **12,** 539–548.

JERO, J., TSENG, C.J., MHATRE, A.N., and LALWANI, A.K. (2001b). A surgical approach appropriate for targeted cochlear gene therapy in the mouse. Hear. Res. **151,** 106–114.

KANZAKI, S., OGAWA, K., CAMPER, S.A., and RAPHAEL, Y. (2002). Transgene expression in neonatal mouse inner ear explants mediated by first and advanced generation adenovirus vectors. Hear. Res. **169,** 112–120.

KANZAKI, S., SHIOTANI, A., INOUE, M., HASEGAWA, M., and OGAWA, K. (2007). Sendai virus vector-mediated transgene expression in the cochlea *in vivo*. Audiol. Neurotol. **12,** 119–126.

KAWAMOTO, K., OH, S.H., KANZAKI, S., BROWN, N., and RAPHAEL, Y. (2001). The function and structural outcome of inner ear gene transfer via the vestibular and cochlear fluids in mice. Mol. Ther. **4,** 575–585.

KELSELL, D.P., DUNLOP, J., STEVENS, H.P., LENCH, N.J., LIANG, J.N., PARRY, G., MUELLER, R.F., and LEIGH, I.M. (1997). Connexin26 mutations in hereditary non-syndromic sensorineural deafness. Nature **387,** 80–83.

KHO, S.T., PETTIS, R.M., MHATRE, A.N., and LALWANI, A.K. (2000). Safety of adeno-associated virus as cochlear gene transfer vector: Analysis of distant spread beyond injected cochleae. Mol. Ther. **2,** 368–373.

KUDO, T., KURE, S., IKEDA, K., XIA, A.P., KATORI, Y., SUZUKI, M., KOJIMA, K., ICHINOHE, A., SUZUKI, Y., AOKI, Y., KOBAYASHI, T., and MATSUBARA, Y. (2003). Transgenic expression of a dominant-negative connexin26 causes degeneration of the organ of Corti and non-syndromic deafness. Hum. Mol. Genet. **12,** 995–1004.

LALWANI, A.K., WALSH, B.J., REILLY, P.G., MUZYCZKA, N., and MHATRE, A.N. (1996). Development of *in vivo* gene therapy for hearing disorders: Introduction of adeno-associated virus into the cochlea of the guinea pig. Gene Ther. **3,** 588–592.

LALWANI, A.K., WALSH, B.J., REILLY, P.G., CARVALHO, G.J., ZOLOTUKHIN, S., MUZYCZKA, N., and MHATRE, A.N. (1998). Long-term *in vivo* cochlear transgene expression mediated by recombinant adeno-associated virus. Gene Ther. **5,** 277–281.

LIU, Y., OKADA, T., SHEYKHOLESLAMI, K., SHIMAZAKI, K., NOMOTO, T., MURAMATSU, S.I., KANAZAWA, T., TAKEUCHI, K., AJALLI, R., MIZUKAMI, H., KUME, A., ICHIMURA, K., and OZAWA, K. (2005). Specific and efficient transduction of cochlear inner hair cells with recombinant adeno-associated virus type 3 vector. Mol. Ther. **12,** 725–733.

LIU, Y., OKADA, T., NOMOTO T., KE X., KUME, A., OZAWA, K., and XIAO, S. (2007). Promoter effects of adeno-associated viral vector for transgene expression in the cochlea *in vivo*. Exp. Mol. Med. **39,** 170–175.

LUEBKE, A.E., FOSTER, P.K., MULLER, C.D., and PEEL, A.L. (2001). Cochlear function and transgene expression in the guinea pig cochlea, using adenovirus- and adeno-associated virus-directed gene transfer. Hum. Gene Ther. **12,** 773–781.

RAPHAEL, Y., FRISANCHO, J.C., and ROESSLER, B.J. (1996). Adenoviral-mediated gene transfer into guinea pig cochlear cells *in vivo*. Neurosci. Lett. **207,** 137–141.

SAMBROOK, J., and RUSSELL, D.W. (2001). Calcium-phosphate-mediated transfection of eukaryotic cells with plasmid DNAs. In: Irwin, N., and Janssen, K.A., eds. *Molecular Cloning: A Laboratory Manual*, 3rd ed. (Cold Spring Harbor Laboratory Press, New York) pp. 16.14–16.20.

STONE, I.M., LURIE, D.I, KELLEY, M.W., and POULSEN, D.J. (2005). Adeno-associated virus-mediated gene transfer to hair cells and support cells of the murine cochlea. Mol. Ther. **11,** 843–848.

SUZUKI, M., YAMASOBA, T., SUZUKAWA, K., and KAGA, K. (2003). Adenoviral vector gene delivery via the round window membrane in guinea pig. Neuroreport **14,** 1951–1955.

YAMADA, M., IWATSUBO, T., MIZUNO, Y., and MOCHIZUKI, H. (2004). Overexpression of α-synuclein in rat substantia nigra results in loss of dopaminergic neurons, phosphorylation of α-synuclein and activation of caspase-9: Resemblance to pathogenetic changes in Parkinson's disease. J. Neurochem. **91,** 451–461.

ZHANG, Y., TANG, W., AHMED, S., SIPP, J.A., CHEN, P., and LIN, X. (2005). Gap junction-mediated intercellular biochemical coupling in cochlear supporting cells is required for normal cochlear functions. Proc. Natl. Acad. Sci. U.S.A. **102,** 15201–15206.

Address reprint requests to:
Dr. Takashi Iizuka
Department of Otorhinolaryngology
Juntendo University School of Medicine
2-1-1 Hongo, Bunkyo-ku
Tokyo 113-8421, Japan

E-mail: t-iizuka@med.juntendo.ac.jp

Received for publication December 6, 2007; accepted after revision February 19, 2008.

Published online: March 26, 2008.

The American Journal of Pathology, Vol. 171, No. 1, July 2007

DOI: 10.2353/ajpath.2007.060948

Neurobiology

Mesenchymal Stem Cell Transplantation Accelerates Hearing Recovery through the Repair of Injured Cochlear Fibrocytes

Kazusaku Kamiya,* Yoshiaki Fujinami,* Noriyuki Hoya,* Yasuhide Okamoto,* Hiroko Kouike,* Rie Komatsuzaki,* Ritsuko Kusano,* Susumu Nakagawa,* Hiroko Satoh,† Masato Fujii,‡ and Tatsuo Matsunaga*

From the Laboratory of Auditory Disorders and Division of Hearing and Balance Research,‡ National Institute of Sensory Organs, and the Department of Plastic Surgery,† National Tokyo Medical Center, Tokyo, Japan*

Cochlear fibrocytes play important roles in normal hearing as well as in several types of sensorineural hearing loss attributable to inner ear homeostasis disorders. Recently, we developed a novel rat model of acute sensorineural hearing loss attributable to fibrocyte dysfunction induced by a mitochondrial toxin. In this model, we demonstrate active regeneration of the cochlear fibrocytes after severe focal apoptosis without any changes in the organ of Corti. To rescue the residual hearing loss, we transplanted mesenchymal stem cells into the lateral semicircular canal; a number of these stem cells were then detected in the injured area in the lateral wall. Rats with transplanted mesenchymal stem cells in the lateral wall demonstrated a significantly higher hearing recovery ratio than controls. The mesenchymal stem cells in the lateral wall also showed connexin 26 and connexin 30 immunostaining reminiscent of gap junctions between neighboring cells. These results indicate that reorganization of the cochlear fibrocytes leads to hearing recovery after acute sensorineural hearing loss in this model and suggest that mesenchymal stem cell transplantation into the inner ear may be a promising therapy for patients with sensorineural hearing loss attributable to degeneration of cochlear fibrocytes. *(Am J Pathol 2007, 171:214–226; DOI: 10.2353/ajpath.2007.060948)*

Mammalian cochlear fibrocytes of the mesenchymal nonsensory regions play important roles in the cochlear physiology of hearing, including the transport of potassium ions to generate an endocochlear potential in the endolymph that is essential for the transduction of sound by hair cells.[1–3] It has been postulated that a potassium recycling pathway toward the stria vascularis via fibrocytes in the cochlear lateral wall is critical for proper hearing, although the exact mechanism has not been definitively determined.[2] One candidate model for this ion transport system consists of an extracellular flow of potassium ions through the scala tympani and scala vestibuli and a transcellular flow through the organ of Corti, supporting cells, and cells of the lateral wall.[4,5] The fibrocytes within the cochlear lateral wall are divided into type I to V based on their structural features, immunostaining patterns, and general location.[5] Type II, type IV, and type V fibrocytes resorb potassium ions from the surrounding perilymph and from outer sulcus cells via the Na,K-ATPase. The potassium ions are then transported to type I fibrocytes, strial basal cells, and intermediate cells through gap junctions and are secreted into the intrastrial space through potassium channels. The secreted potassium ions are incorporated into marginal cells by the Na,K-ATPase and the Na-K-Cl co-transporter, and are finally secreted into the endolymph through potassium channels.

Degeneration and alteration of the cochlear fibrocytes have been reported to cause hearing loss without any other changes in the cochlea in the Pit-Oct-Unc (POU)-domain transcription factor Brain-4 (Brn-4)-deficient mouse[6] and the otospiralin-deficient mouse.[3] *Brn-4* is the gene responsible for human DFN3, an X chromosome-linked nonsyndromic hearing loss. Mice deficient in Brn-4 exhibit reduced endocochlear potential and hearing loss and show severe ultrastructural alterations, including cel-

Supported by the Ministry of Health, Labor, and Welfare of Japan (health science research grant H16-kankakuki-006 to T.M.) and the Japan Foundation for Aging and Health (to K.K.).

Accepted for publication March 26, 2007.

Address reprint requests to Dr. Tatsuo Matsunaga, Laboratory of Auditory Disorders, National Institute of Sensory Organs (NISO), National Tokyo Medical Center, 2-5-1 Higashigaoka, Meguro-ku, Tokyo 152-8902, Japan. E-mail: matsunagatatsuo@kankakuki.go.jp.

lular atrophy and a reduction in the number of mitochondria, exclusively in spiral ligament fibrocytes.[6,7] In the otospiralin-deficient mouse, degeneration of type II and IV fibrocytes is the main pathological change, and hair cells and the stria vascularis appear normal.[3] Furthermore, in mouse and gerbil models of age-related hearing loss,[8–10] degeneration of the cochlear fibrocytes precede the degeneration of other types of cells within the cochlea, with notable pathological changes seen especially in type II, IV, and V fibrocytes. In humans, mutations in the connexin 26 (*Cx26*) and connexin 30 (*Cx30*) genes, which encode gap junction proteins and are expressed in cochlear fibrocytes and nonsensory epithelial cells, are well known to be responsible for hereditary sensorineural deafness.[11,12] These instances of deafness related to genetic, structural, and functional alterations in the cochlear fibrocytes highlight the functional importance of these fibrocytes in maintaining normal hearing.

Recently, we developed an animal model of acute sensorineural hearing loss attributable to acute cochlear energy failure by administering the mitochondrial toxin 3-nitropropionic acid (3NP) into the rat round window niche.[13,14] 3NP is an irreversible inhibitor of succinate dehydrogenase, a complex II enzyme of the mitochondrial electron transport chain.[15,16] Systemic administration of 3NP has been used to produce selective striatal degeneration in the brain of several mammals.[17,18] Our model with 3NP administration into the rat cochlea showed acute sensorineural hearing loss and revealed an initial pathological change in the fibrocytes of the lateral wall and spiral limbus without any significant damage to the organ of Corti or spiral ganglion. Furthermore, depending on the dose of 3NP used, these hearing loss model rats exhibited either a permanent threshold shift or a temporary threshold shift. In the present study, we used doses of 3NP that induce temporary threshold shift to explore the mechanism of hearing recovery after injury to the cochlear fibrocytes and examined a novel therapeutic approach to repair the injured area using mesenchymal stem cell (MSC) transplantation.

MSCs are multipotent cells that can be isolated from adult bone marrow and can be induced to differentiate into a variety of tissues *in vitro* and *in vivo*.[19] Human MSCs transplanted into fetal sheep intraperitoneally undergo site-specific differentiation into chondrocytes, adipocytes, myocytes, cardiomyocytes, bone marrow stromal cells, and thymic stroma.[20] Furthermore, when MSCs were transplanted into postnatal animals, they could engraft and differentiate into several tissue-specific cell types in response to environmental cues provided by different organs.[21] These transplantability features of MSCs suggested the possibility that they could restore hearing loss in 3NP-treated rats to the normal range. Recently, experimental bone marrow transplantation into irradiated mice suggested that a part of spiral ligament that consists of cochlear fibrocytes was derived from bone marrow cells or hematopoietic stem cells.[22] This indicates that bone marrow-derived stem cells such as MSCs may have a capacity to repair the injury of cochlear fibrocytes. In this study, we demonstrate that MSC transplantation significantly improves hearing recovery, and present evidence suggesting invasion of transplanted MSCs into the injured region of the cochlear lateral wall and repair of the interrupted gap junction network.

Materials and Methods

Rat Model of Acute Sensorineural Hearing Loss Attributable to Cochlear Fibrocyte-Specific Injury

Experimental procedures reported in this study were approved by the Institutional Animal Care and Use Committee of the National Tokyo Medical Center. Sprague-Dawley rats (Clea Japan, Tokyo, Japan) weighing between 180 and 210 g (8 to 10 weeks old) were used. Before surgery, the animals were anesthetized with pentobarbital (30 to 40 mg/kg, i.p.; Dainippon Pharmaceutical, Osaka, Japan), and after local administration of 1% lidocaine (AstraZeneca PLC, London, UK), an incision was made posterior to the left pinna near the external meatus. The left otic bulla was opened to approach the round window niche. The distal end of a section of PE 10 tubing (Becton-Dickinson, Franklin Lakes, NJ) was drawn to a fine tip in a flame and gently inserted into the round window niche. 3NP (Sigma, St. Louis, MO) was dissolved in saline at 300 mmol/L and the pH adjusted to 7.4 with NaOH. Saline alone was used as a control. The solution was administered for 2 minutes at a rate of 1.5 μl/minute with a syringe pump. After treatment, a small piece of gelatin was placed on the niche to keep the solution in the niche regardless of head movement, and the wound was closed. The right cochlea was surgically destroyed to avoid cross-hearing during auditory brainstem response (ABR) recording.

Auditory Brainstem Response

ABR recording was performed as previously described[13] before surgery and at 2 hours and 1, 2, 3, 7, 14, 21, 28, 35, and 42 days after surgery (or until 14 days in the MSC transplantation experiment). Six to 12 rats in each group were used for the recordings. ABR was recorded using Scope waveform storing and stimulus control software and the PowerLab data acquisition and analysis system (PowerLab2/20; AD Instruments, Castle Hill, Australia). Electroencephalogram recording was performed using a digital Bioamp extracellular amplifier system (BAL-1; Tucker-Davis Technologies, Alachua, FL). Sound stimuli were produced by a coupler type speaker (ES1spc; Bio Research Center, Nagoya, Japan) inserted into the ear canal. Pure tone bursts of 8, 20, and 40 kHz (0.2-ms rise/fall time and 1-ms flat segment) were generated, and the amplitude was specified by a real-time processor and programmable attenuator (RP2.1 and PA5; Tucker-Davis Technologies). Sound level calibration and frequency confirmation were performed using a 1/4 inch free-field mic (7016; ACO Pacific, Belmont, CA), microphone amp (MA3; Tucker-Davis Technologies), a digital oscilloscope (DS-8822P; Iwatsu Electronic, Tokyo, Japan), and a sound level meter (NL32; Rion, Tokyo, Japan). The maximum output level was 87, 86, and 96 dB at 8, 20, and 40

kHz, respectively. For recording, the animals were anesthetized with pentobarbital before stainless steel needle electrodes were placed ventrolateral to the ears. Waveforms of 512 stimuli at a frequency of 9 Hz were averaged, and the visual detection threshold was determined by increasing or decreasing the sound pressure level in 5-dB steps. The effects of 3NP and/or MSC transplantation on the ABR threshold and recovery ratio of ABR threshold (peak threshold − threshold at 14 days or 42 days/peak threshold × 100) were statistically analyzed at each frequency using an unpaired Student's *t*-test. The significance level for all statistical procedures was set at $P < 0.05$.

Bromodeoxyuridine (BrdU) Injection

To detect cell proliferation in the rat inner ear, BrdU (Sigma) was injected (30 mg/kg i.p. per single injection) as previously described.[23] Injections were started just after 3NP administration and continued every 12 hours for 3 or 6 days.

MSC Preparation

We previously established bone marrow MSCs and demonstrate their potential to differentiate into several cell types.[24] The cells were prepared from 6- to 8-week-old male F344 rats (Clea) as described. In brief, surgical treatment was performed after intraperitoneal injection of pentobarbital (30 to 40 mg/kg, i.p.). After surgery, the rats were sacrificed by ether inhalation followed by dislocation of the neck. Rat femurs and tibiae were collected and the long bones meticulously dissected to remove all adherent soft tissue. Both ends of the bones were cut away from the diaphyses with bone scissors. The bone marrow plugs were hydrostatically expelled from the bones by inserting 18-gauge needles fastened to 10-ml syringes filled with complete medium [Dulbecco's modified Eagle's medium (Sigma), 10% fetal bovine serum (Sigma), and 100 U/ml penicillin-streptomycin (Sigma)] into the distal ends of the femora and the proximal ends of the tibiae. Cells were plated on plastic culture dishes. The nonadherent cell population was removed after 24 hours, and the adherent layer was washed once with fresh media. The cells were then continuously cultured for 1 to 4 weeks in complete medium. Medium was completely replaced every 3 days. When the cells were nearly confluent, the adherent cells were released from the dishes with 0.25% trypsin-ethylenediaminetetraacetic acid (Sigma), split 1:3, and seeded onto fresh plates. Cells from passages 10 to 15 were stored with Cell Banker reagent (Juji Field, Tokyo, Japan) in liquid nitrogen. The frozen cell suspensions were thawed at 1 week before the transplantation and cultured in complete medium at 37°C in a humidified atmosphere of 5% CO_2. The potential of these cells as MSCs were previously demonstrated as described.[24] The surface marker expression of these cells was analyzed by flow cytometry (Epics Altra with HyPerSort cell sorting system; Beckman Coulter, Fullerton, CA). At ~80 to 90% confluence, MSCs were dissociated by treatment with 1× Accutase (Chemicon International, Temecula, CA) for 15 minutes at 37°C followed by phosphate-buffered saline (PBS) washout, centrifugation at 1200 rpm for 10 minutes, and resuspension in Hanks' balanced salt solution $(HBSS)^+$ medium [$HBSS^-$ medium (Invitrogen Japan, Tokyo, Japan) with 2% fetal bovine serum and 10 mmol/L 2-[4-(2-hydroxyethyl)-1-piperazinyl]ethanesulfonic acid (HEPES) buffer (Invitrogen Japan)]. MSCs were incubated with antibodies against CD45, CD31, CD29, CD44H, CD54, CD73, and CD90 (BD PharMingen, San Diego, CA) for 30 minutes on ice and spun down. At the end of the staining, MSCs were resuspended in ice-cold $HBSS^+$ medium containing 2 μg/ml propidium iodide for discrimination of dead cells. To detect the MSCs after injection, cultured MSCs were incubated with 5 μmol/L BrdU for 2 days before transplantation as previously described.[25]

MSC Transplantation

Before transplantation, cultured MSCs were released from the dishes with 0.25% trypsin-ethylenediaminetetraacetic acid and washed by centrifugation with Dulbecco's phosphate-buffered saline (D-PBS; Invitrogen Japan) and resuspended to prepare MSC suspension (1×10^5 cells in 20 μl of D-PBS) for the following transplantation. Three days after 3NP administration, the rats were anesthetized with pentobarbital (30 to 40 mg/kg, i.p.) and by local administration of 1% lidocaine. Incisions were made as described for 3NP administration, the surfaces of the posterior and lateral semicircular canals were exposed, and a small hole was made in each canal. A small tube (Eicom, Kyoto, Japan) was inserted into the lateral semicircular canal toward the ampulla. Through this tube, the perilymph was perfused with an MSC suspension (1×10^5 cells in 20 μl of D-PBS) for 10 minutes at a rate of 2 μl/minute using a syringe pump with drainage from the hole made on the posterior semicircular canal. The tube was then removed, the holes on the semicircular canals were sealed with a muscle and fibrin adhesive (Beriplast P Combi-set; CSL Behring, King of Prussia, PA), and the wound on the neck was closed. An equal volume of vehicle (D-PBS) was also injected into the semicircular canal of 3NP-treated rats as control.

Tissue Preparation

The rats were sacrificed at 3 days (three rats for 3NP and three rats for saline control) and 42 days (five rats for 3NP and three rats for saline control) after 3NP treatment and 11 days after MSC transplantation (12 rats for 3NP with MSC transplantation, seven rats for MSC transplantation only, and five rats for 3NP followed by vehicle injection). They were deeply anesthetized with pentobarbital and transcardially perfused with 0.01 mol/L phosphate buffer, pH 7.4, containing 8.6% sucrose followed by a fixative consisting of freshly depolymerized 4% paraformaldehyde in 0.1 mol/L phosphate buffer (pH 7.4). After decapitation, the left temporal bones were removed and immediately placed in the same fixative. Small openings

were made at the round window, oval window, and the apex of the cochlea. After overnight immersion in fixative, the temporal bones were decalcified by immersion in 5% sucrose, 5% ethylenediaminetetraacetic acid, pH 7.4, with stirring at 4°C for 14 days. The specimens were dehydrated through graded concentrations of alcohol, embedded in paraffin blocks, and sectioned into 5-μm-thick slices. The sections were stained with hematoxylin and eosin (H&E) as generally described, by terminal deoxynucleotidyl transferase (TdT)-mediated dUTP nick-end labeling (TUNEL) and by immunohistochemistry for BrdU, Cx30, or Cx26 as described below.

TUNEL Assay

TUNEL assays were performed using an ApopTag Fluorescein Direct *in situ* apoptosis detection kit (Chemicon International) according to the manufacturer's instructions. In brief, specimens were digested with 20 μg/ml proteinase K in 0.01 mol/L PBS, pH 7.4, for 5 minutes, incubated with TdT and fluorescein-labeled nucleotide in a humid atmosphere at 37°C for 1 hour, and then incubated with 2 μmol/L TOPRO-3 iodide (Molecular Probes, Eugene, OR) for 5 minutes. The specimens were viewed with a confocal laser microscope (LSM510; Carl Zeiss, Esslingen, Germany; or Radiance 2100; Bio-Rad, Hercules, CA), and each image was analyzed and saved by ZeissLSM image browser (Carl Zeiss). Negative controls included proteinase K digestion but did not include TdT so that nonspecific incorporation of nucleotide, or nonspecific binding of enzyme-conjugate, could be assessed. Distilled water was substituted for TdT enzyme reagent in negative controls.

Immunohistochemistry

After pretreatment with 2 mol/L HCl at 37°C for 30 minutes, incubation with 20 μg/ml proteinase K in PBS for 5 minutes, and incubation with blocking solution (1.5% normal goat serum in PBS) for 30 minutes at room temperature, tissue sections were incubated with anti-BrdU antibody (DAKO, Glostrup, Denmark) diluted 1:100 in PBS for 30 minutes, then with biotin-conjugated anti-mouse IgG (Vector, Burlingame, CA) diluted 1:200 in PBS for 30 minutes, followed by horseradish peroxidase (HRP)-conjugated streptavidin-biotin complex (streptABComplex-HRP, Vectastain Elite ABC kit standard; Vector) for 1 hour at room temperature. Sections were stained in DAB-H_2O_2 (Vector) for 3 minutes and hematoxylin for 1 minute and then rinsed and covered with a coverslip. For BrdU and TUNEL double staining, Alexa568-conjugated anti-mouse IgG (1:600; Molecular Probes) was used as a secondary antibody in the BrdU staining after the TUNEL procedure. For double-staining of BrdU with Cx30 or Cx26, rabbit anti-Cx26 (1:300; Zymed Laboratories, South San Francisco, CA) or rabbit anti-Cx30 (1:400; Zymed Laboratories) antibody and anti-BrdU antibody were used as a primary antibody cocktail, and Alexa488-conjugated anti-rabbit IgG (1:400; Molecular Probes) with Alexa568-conjugated anti-mouse IgG were used as a secondary antibody cocktail. For nuclear staining, TO-PRO-3 iodide (2 μmol/L; Molecular Probes), 4,6-diamidino-2-phenylindole (1 μg/ml; Dojindo Laboratories, Kumamoto, Japan) or propidium iodide (1 μg/ml; Molecular Probes) was used. Negative controls were performed without primary antibodies to assess nonspecific binding of the secondary antibody or of the streptAB-Complex-HRP. Inner ear sections that were not injected with BrdU were also used as negative controls. Background autofluorescence was not observed in the cochlear sections with the tissue preparation methods used in the present study.

Results

Long-Term Observation of Temporary Threshold Shift and Hearing Recovery after 3NP Administration

We monitored ABR thresholds in 3NP-treated rats at 8, 20, and 40 kHz for 42 days after 3NP administration (Figure 1, A–C) to examine the potential for hearing recovery. At all frequencies, the ABR thresholds peaked 1 day after 3NP administration and then gradually recovered. At 8 kHz (n = 7), the threshold reached within a normal threshold level (11 dB) 42 days after 3NP administration. However, the ABR threshold at 40 kHz showed only a mild recovery after 14 days. The hearing recovery ratio, which is described in Materials and Methods, was calculated for each tested frequency (Figure 1D). At 14 days, the recovery ratios were 73.4 ± 5.5% for 8 kHz (n = 11), 57.0 ± 11.2% for 20 kHz (n = 11), and 37.5 ± 7.7% for 40 kHz (n = 12). At 42 days, they were 97.2 ± 9.4% for 8 kHz (n = 7), 67.0 ± 16.4% for 20 kHz (n = 7), and 32.3 ± 7.7% for 40 kHz (n = 7). Throughout the recovery time course, the recovery ratios at the lower frequencies always tended to be higher than those at the highest frequency. At 42 days, the recovery ratio for 8 kHz was significantly higher than that for 40 kHz (P = 0.005). Between 14 and 42 days after 3NP administration, the hearing level for 40 kHz did not show significant recovery, but the recovery ratios for 8 and 20 kHz showed 24 and 10% increases, respectively.

Apoptosis and Regeneration of the Cochlear Fibrocytes after 3NP Administration

To analyze the pathological changes associated with the acute hearing loss observed in the 3NP-treated rats, we performed H&E staining and TUNEL reaction to detect apoptosis. No histological changes were observed in the organ of Corti and spiral ganglion of rats with 3NP administration as shown in Figure 2, A and B. However, severe apoptosis, with chromatin condensation and apoptotic bodies, was observed only in the lateral wall and the spiral limbus at 3 days after 3NP administration (Figure 2, C and D). These severe apoptotic regions included more than 30% TUNEL-positive or apoptotic cells and were clearly demarcated as shown in Figure 2,

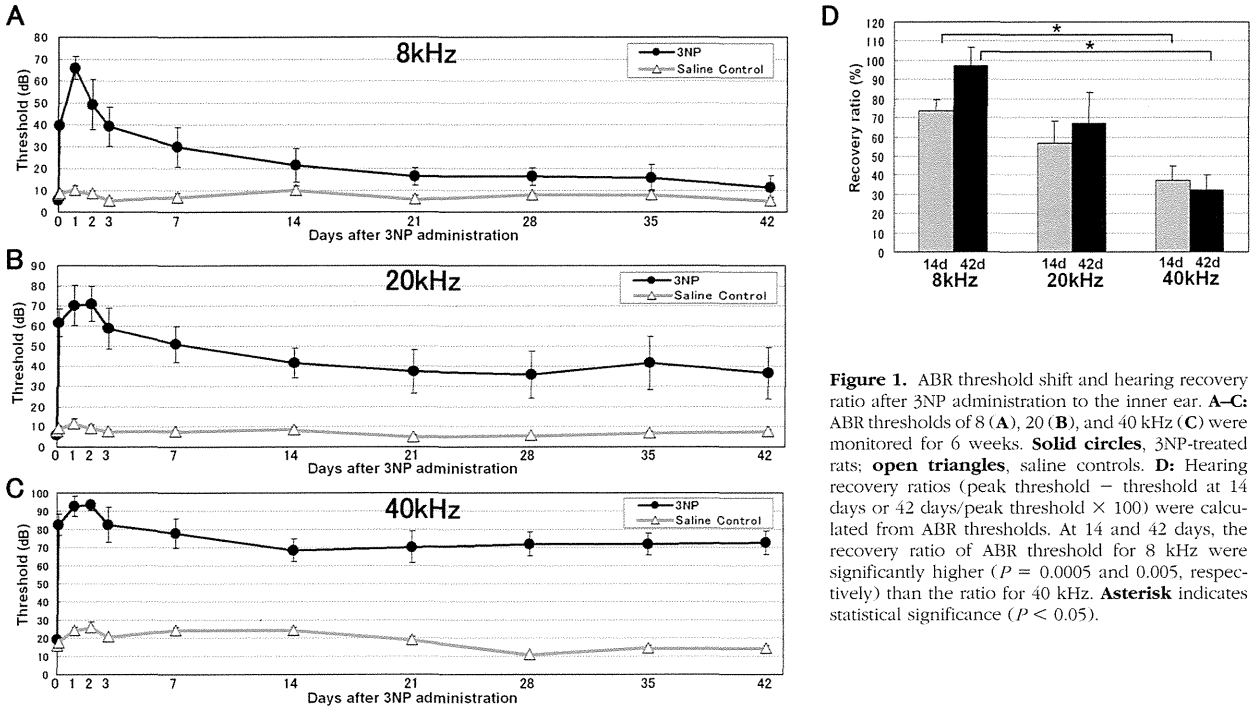

Figure 1. ABR threshold shift and hearing recovery ratio after 3NP administration to the inner ear. **A–C:** ABR thresholds of 8 (**A**), 20 (**B**), and 40 kHz (**C**) were monitored for 6 weeks. **Solid circles**, 3NP-treated rats; **open triangles**, saline controls. **D:** Hearing recovery ratios (peak threshold − threshold at 14 days or 42 days/peak threshold × 100) were calculated from ABR thresholds. At 14 and 42 days, the recovery ratio of ABR threshold for 8 kHz were significantly higher ($P = 0.0005$ and 0.005, respectively) than the ratio for 40 kHz. **Asterisk** indicates statistical significance ($P < 0.05$).

E and F. These areas contain cochlear fibrocytes that participate in the potassium recycling route within the cochlea. The typical distribution pattern of TUNEL-positive cells after 3NP treatment is shown in Figure 2E, but a few rats with more severe hearing impairment (with ~55 dB elevation of the ABR threshold) demonstrated more prominent histological changes, with focal cell loss in the center surrounded by TUNEL-positive cells (Figure 2, G and H). On light microscopic observation of H&E-stained sections, histological changes suggesting inflammation were not evident in the lateral wall and spiral limbus. As for cochlear turns, lateral wall in basal turn had more severe damage than the middle turn as shown in Figure 4, G, I, and J, and the apical turn had little damage in the lateral wall.

To analyze the mechanism of hearing recovery after damage to the cochlear lateral wall, we performed a BrdU incorporation assay in addition to the TUNEL assay (Figure 3). BrdU-positive cells were observed mainly in the lateral wall fibrocytes and occasionally observed in spiral limbus, Schwann cells, and Reissner's membrane. At 3 days after 3NP administration, the BrdU-positive cell count around the area of apoptosis in the lateral wall was 6.2 ± 0.7 cells (19 cross sections from three rats) compared with 0.5 ± 0.1 cells (12 cross sections from three rats) for the control (Figure 3, A–C). Furthermore, a few TUNEL-positive dying cells that take up BrdU were detected, indicating that some fibrocytes that regenerated after 3NP administration also became apoptotic 3 days after 3NP administration (Figure 3C, arrow). To trace the cells regenerated after the early injury, the rats were continuously injected with BrdU during the first 6 days after 3NP administration and sacrificed 42 days after 3NP administration for detection of BrdU-positive cells. Few TUNEL-positive cells were detected, but a number of BrdU-positive cells could be detected in the central part of the lateral wall in the middle turn of the cochlea (Figure 3, D–F). At 42 days after 3NP administration, 2.6 ± 0.8 BrdU-positive cells were detected in a cross section of the lateral wall of the middle turn in 3NP-treated rats (26 cross sections from five rats) compared with 0.2 ± 0.2 cells in saline-treated controls (12 cross sections from three rats). In contrast, only a few BrdU-positive cells were detected in the spiral limbus at 3 and 42 days after 3NP administration.

Characterization of MSCs

For the MSC transplantation into inner ear, we used rat bone marrow-derived cells, which we previously established and demonstrated their capacity for differentiation as MSC.[24] Flow cytometry of these MSCs before the transplantation demonstrated surface expression of CD29, CD44H, CD54, CD73, and CD90, but not of CD31 or CD45. This surface expression pattern was similar to human and murine MSCs.[26,27]

Transplantation and Detection of MSCs in the Inner Ear Tissue

To improve the hearing recovery of high-frequency (40 kHz) sounds, we transplanted BrdU-labeled MSCs into the inner ear of 3NP-treated rats using perilymphatic perfusion with MSC suspension from the lateral semicircular canal. Eleven days after transplantation, a number of BrdU-positive cells were observed along the ampullary crest surface facing the perilymph in the lateral semicircular canal that was closest to the site of MSC injection (Figure 4A, arrow), suggesting that the transplanted

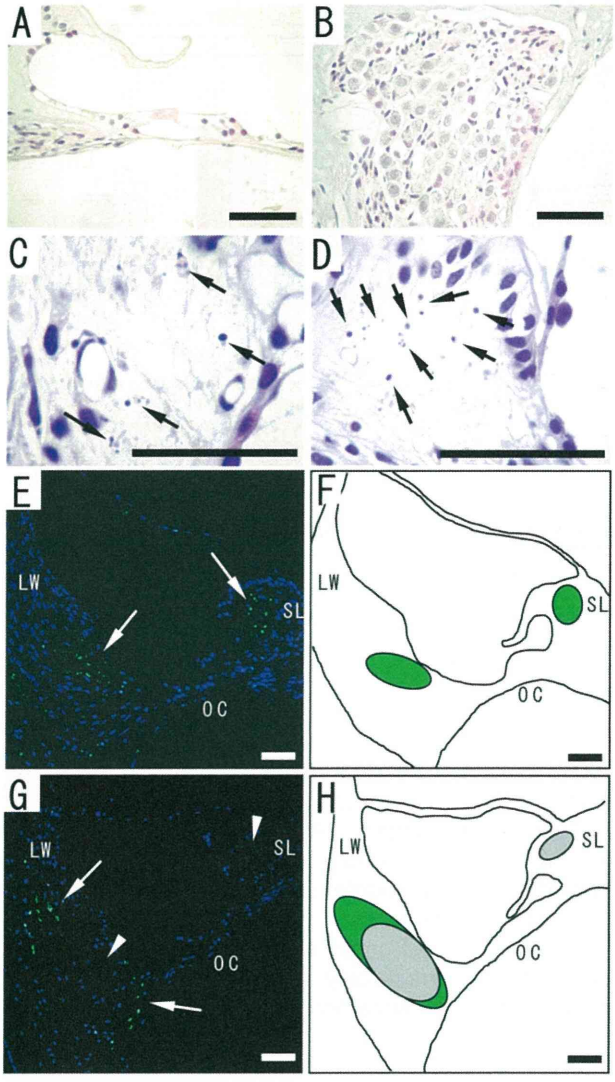

Figure 2. Apoptosis in the rat cochlea at 3 days after 3NP administration. **A–D:** H&E staining of the cochlea. Severe focal apoptosis showing chromatin condensation and apoptotic bodies (**arrows**) was observed in the lateral wall (**C**) and the spiral limbus (**D**), whereas no morphological changes were observed in the organ of Corti (**A**) and the spiral ganglion (**B**). **E** and **G:** TUNEL staining (green) of the cochlea in rats showing moderate (~35 dB elevation of ABR threshold for 8 kHz, **E**) and severe (~55 dB elevation of ABR threshold for 8 kHz, **G**) hearing impairment. **E:** The areas of apoptosis indicated by TUNEL-positive cells (**arrows**) were clearly demarcated in the lateral wall and spiral limbus. Nuclei were stained by TOPRO-3. **G:** Acellular areas (**arrowheads**) corresponded to the apoptotic areas in **E**, and severe apoptosis was observed in the area around the acellular site (**arrows**). Schematic illustration of the areas of apoptosis and cell loss in **E** and **G** are shown in **F** and **H**, respectively. Areas of apoptosis including more than 30% of TUNEL-positive cells or apoptotic cells are indicated in green, and areas of loss of fibrocytes are indicated in gray. SL, spiral limbus; LW, lateral wall; OC, organ of Corti. Scale bars = 50 μm.

MSCs survived there even 11 days after injection. Some of these BrdU-positive cells were attached to the surface of the ampullary crest (Figure 4B, asterisk) and a number of cells had invaded the tissue (Figure 4B, arrow) although a few of the invading cells displayed morphological features suggesting rejection by the host tissue. Aggregations of MSCs were frequently observed on the bone surface in the scala tympani (Figure 4, C and D). In the apical part of the lateral wall facing the scala vestibuli, a number of BrdU-positive cells were detected within the tissue (Figure 4E). These cells showed the morphological features of pretransplantation MSCs, ie, large and round (Figure 4F). Many BrdU-positive cells were also observed in the middle part of the lateral wall (Figure 4G) injured by 3NP treatment. The shape of these MSCs resembled that of the cochlear fibrocytes. In the hook region of the cochlea, a large number of BrdU-positive cells were also detected in the area neighboring the lateral wall injury (Figure 4, H and I). In the lateral wall of the middle turn, BrdU-positive cells were occasionally observed without a loss of fibrocytes in the corresponding area, suggesting that the MSCs that had invaded the lateral wall supplemented the injured area to repair damage (Figure 4J). In contrast to the lateral wall, only a few BrdU-positive cells were detected in the spiral limbus (Figure 4K, arrow). No morphological changes were observed in any cochlear hair cells in every group.

We used 12 3NP-treated rats and seven nontreated rats for BrdU-labeled MSC transplantation. BrdU-positive cells were detected in all of the inner ear tissues of the examined rats. Successful invasion of the lateral wall by MSCs was observed in 6 of the 12 rats treated with 3NP and one of the seven control rats (Table 1). Thus, the rats with lateral wall injury had a higher rate of MSC invasion of the lateral wall than those without injury. BrdU-positive cells were counted in five cross sections of the cochlear middle turn in each rat that showed invasion of MSCs into the lateral wall after 3NP and MSC treatment, and the approximate mean values of BrdU-positive cells observed in a cross section of the cochlear middle turn distributed between 11 and 15 in scala tympani, between 6 and 10 in apical part of lateral wall, middle part of lateral wall, and scala vestibuli, less than one in spiral limbus, and not detected in the organ of Corti and the spiral ganglion.

Expression of Gap Junction Proteins in Transplanted MSCs

To investigate the functional contribution of MSCs detected in injured and uninjured areas of the lateral wall, we analyzed expression of the gap junction proteins Cx30 and Cx26 in the transplanted MSCs. Gap junctions between cochlear fibrocytes play an important role in the cochlear potassium recycling system, and breaks in the gap junction network because of loss of fibrocytes are thought to be a main cause of the 3NP-induced hearing loss. In both normal and 3NP-treated rats, both Cx30 and Cx26 had the same expression pattern in most fibrocytes of the whole part of the lateral wall. Immunostaining for Cx30 or Cx26 showed punctuate cytoplasmic staining and strong spots of staining mainly at the sites of attachment to adjacent fibrocytes (Figure 5, A–L). All of the MSCs invaded into the lateral wall showed the expression of Cx30 and Cx26. The expression patterns of Cx30 and Cx26 in cochlear fibrocytes were the same between apical part and middle part of lateral wall, but only the invaded MSCs in the apical part of lateral wall showed different expression patterns. The MSCs detected in the apical part also expressed Cx30 and Cx26; however,

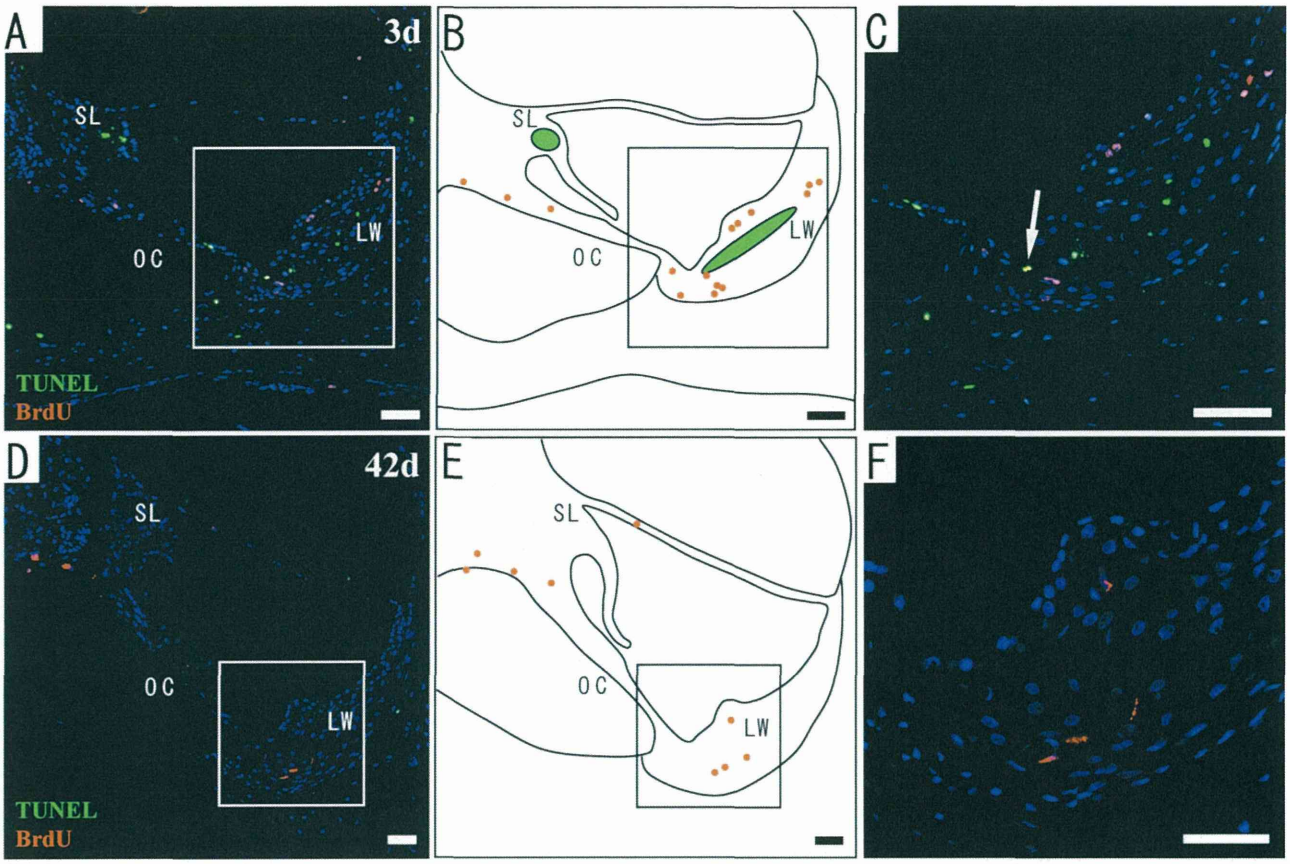

Figure 3. Regeneration and apoptosis of rat cochlear fibrocytes after 3NP administration. Double staining of BrdU (red) and TUNEL (green) assay 3 days (**A–C**) and 42 days (**D–F**) after 3NP administration. **B** and **E:** Schematic illustration for **A** and **D**. Green areas indicate the areas of apoptosis and red points indicate BrdU-positive cells. **C** and **F:** Higher magnification of the squared areas in **A** and **D**. A BrdU- and TUNEL-double-positive cell (yellow) was also observed (**arrow**). Nuclei (blue) were stained by TOPRO-3. SL, spiral limbus; LW, lateral wall; OC, organ of Corti. Scale bars = 50 μm.

expression of Cx30 was very weak (Figure 5, A–C), and these cells did not show the punctate staining pattern at the site of contact with neighboring fibrocytes suggestive of gap junction connections (Figure 5C). Likewise, Cx26 staining spots at attachment sites to neighboring fibrocytes were not clearly observed (Figure 5, D–F). The transplanted MSCs occasionally displayed a morphology of dividing cell, suggesting that the MSCs can proliferate after their invasion into the lateral wall (Figure 5B). In contrast, within the middle part of the lateral wall near the injured region, most of the BrdU-positive cells and neighboring BrdU-negative fibrocytes strongly and similarly expressed Cx30 in the cytoplasm (Figure 5, G–I). In this area, Cx26 was also expressed by BrdU-positive cells in a similar staining pattern to BrdU-negative neighboring fibrocytes (Figure 5, J–L). BrdU-positive cells were observed even in the area where fibrocytes were not found (ie, the area without blue nuclear staining) and demonstrated Cx26 expression at the tips of their cytoplasmic processes (Figure 5, K and L; arrowheads). Moreover, these cells occasionally showed a morphology of the dividing cell (Figure 5, K and L; arrows). Nuclei of some MSCs appeared small and irregular, but signs of apoptosis such as fragmentation of nuclei were not detected in such MSCs. In addition, MSCs showed immunostaining of both Cx30 and Cx26 not only in cytoplasm and cell membrane but also in a part of nucleus, although these proteins were not distributed in nuclei of normal cochlear fibrocytes (Figure 5, C, F, I, and L).

A summary of the histological observations shown in Figures 2, 4, and 5 and our hypothesis for the movement of transplanted MSCs are represented in the schematic illustration in Figure 6. In brief, after the perilymphatic perfusion with MSC suspension, MSCs settled on the surface of the scala tympani and the scala vestibuli within the cochlea. The injuries to cochlear fibrocytes caused by 3NP induced secretion of some chemokines from the injured area. With these stimulating signals, MSCs in the scala vestibuli invaded the lateral wall while maintaining their round shape. Then these MSCs migrated toward the injured area while maintaining the capacity for proliferation. The MSCs that reached the injured area continued to proliferate and repaired the disconnected gap junction network.

Acceleration of Hearing Recovery by MSC Transplantation

To evaluate the effect of MSC transplantation on hearing recovery in 3NP-treated rats, we monitored the ABR thresholds for 2 weeks after 3NP administration. In rats in which MSCs were transplanted without previous 3NP treatment (Figure 7, A–C), no significant threshold shift was recorded,

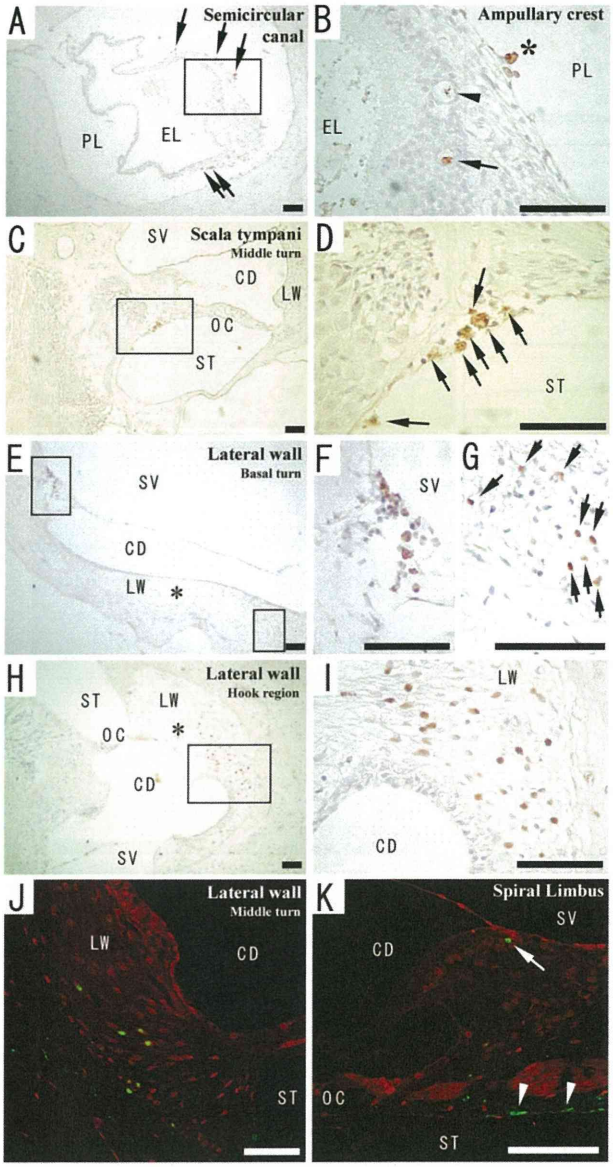

Figure 4. MSCs prelabeled with BrdU and transplanted into the inner ear of 3NP-treated rats at 11 days after the transplantation. **B**, **D**, **F**, **G**, and **I** are high-magnification images of the squared area of the left panels (**A**, **C**, **E**, and **H**). A number of BrdU-positive cells were observed (**A**, **arrows**), and some BrdU-positive cells were attached to the surface of the ampullary crest (**B**, **asterisk**) or had invaded the tissue (**B**, **arrow**). An **arrowhead** indicates BrdU-positive cells that appeared to be rejected by the recipient tissue. **C** and **D:** In the scala tympani, a mass of MSCs (**arrows**) was observed on the bone surface. In the cochlear lateral wall, MSCs were detected within the tissue (**E**, **asterisk** indicates the injured area). A number of MSCs were detected in the apical part of the lateral wall (**F**), and many MSCs were detected within the injured area of the cochlear lateral wall (**G**, **arrows**). **H** and **I:** A large number of BrdU-positive cells were detected near the injured area (**asterisk**) of the lateral wall at the hook region of the cochlea. **J** and **K:** Immunofluorescent staining of MSCs in the middle turn of cochlea. Only one MSC was observed in the spiral limbus (**K**, **arrow**). **Arrowheads** indicate MSCs that appear to be attached to the surface of the basilar membrane. Nuclei were stained with propidium iodide (red). PL, perilymph; EL, endolymph; SV, scala vestibuli; CD, cochlear duct; ST, scala tympani; LW, lateral wall; OC, organ of Corti. Scale bars = 50 μm.

indicating that there was no significant hearing loss caused by the transplantation operation itself. Of the 12 rats that received MSC transplantation after 3NP treatment, the six rats who demonstrated MSC invasion of the lateral wall by

Table 1. Number of Rats in Which Mesenchymal Stem Cells (MSCs) Were Observed in the Cochlear Tissue 11 Days after MSC Transplantation

	Rats tested	MSC survival	Invasion into lateral wall
3NP + MSC	12	12	6
MSC only	7	7	1

3NP + MSC, rats in which MSC transplantation was performed 3 days after administration of 3NP; MSC only, control rats into which MSCs were transplanted without previous 3NP administration; MSC survival, the number of rats in which surviving MSCs were detected within the cochlea; and invasion into lateral wall indicates the number of rats showing MSC invasion into the lateral wall.

histological analysis, and thus were most likely to experience recovery of hearing, were selected for ABR data collection. At 14 days after 3NP administration, the ABR thresholds both of rats receiving MSC transplantation after 3NP treatment (3NP + MSC, $n = 12$ for 8 and 20 kHz and $n = 7$ for 40 kHz) and of 3NP-treated rats that demonstrated MSC invasion of the lateral wall (3NP + MSC/LW, $n = 6$ for 8 and 20 kHz and $n = 3$ for 40 kHz) selected from 3NP + MSC in the following histochemical analysis were lower than those of 3NP-treated rats without MSC transplantation (Figure 7, A–C) for 8, 20, and 40 kHz. A remarkable decrease in the ABR threshold at 40 kHz was detected in 3NP-treated rats with MSC invasion of the lateral wall compared with the 3NP-treated group lacking transplantation at 14 days, although little difference had been seen at 7 days (Figure 7C). This result suggests that an even greater effect on the ABR threshold by MSC transplantation may be expected with a longer observation period. The 3NP-treated rats with MSC transplantation also had higher recovery ratios than the 3NP-treated rats without MSC transplantation at all tested frequencies 14 days after 3NP administration (Figure 7D). Moreover, the rats with lateral wall invasion of MSCs tended to show a higher recovery ratio than the other two groups. The difference between the 3NP-treated rats showing invasion of MSC into the lateral wall and 3NP-treated rats without transplantation was greater for higher frequencies: at 40 kHz, the recovery ratio was significantly higher (~23%, $P = 0.036$) for the rats with lateral wall invasion of MSCs. To examine the effect of surgical manipulation, an equal volume of vehicle (D-PBS) was also injected into the semicircular canal of 3NP-treated rats as control. These control experiments showed that the vehicle injection did not change the time course of ABR thresholds at 8 kHz but aggravated the ABR thresholds at 20 kHz at 7 days after 3NP administration and aggravated the ABR thresholds at 40 kHz at least at 7 and 14 days after 3NP administration in comparison with 3NP-treated rats with or without MSC transplantation.

Discussion

Apoptosis and Regeneration of Cochlear Fibrocytes in 3NP-Treated Rats

In this study, we demonstrated that acute hearing loss in rats treated with the mitochondrial toxin 3NP corre-

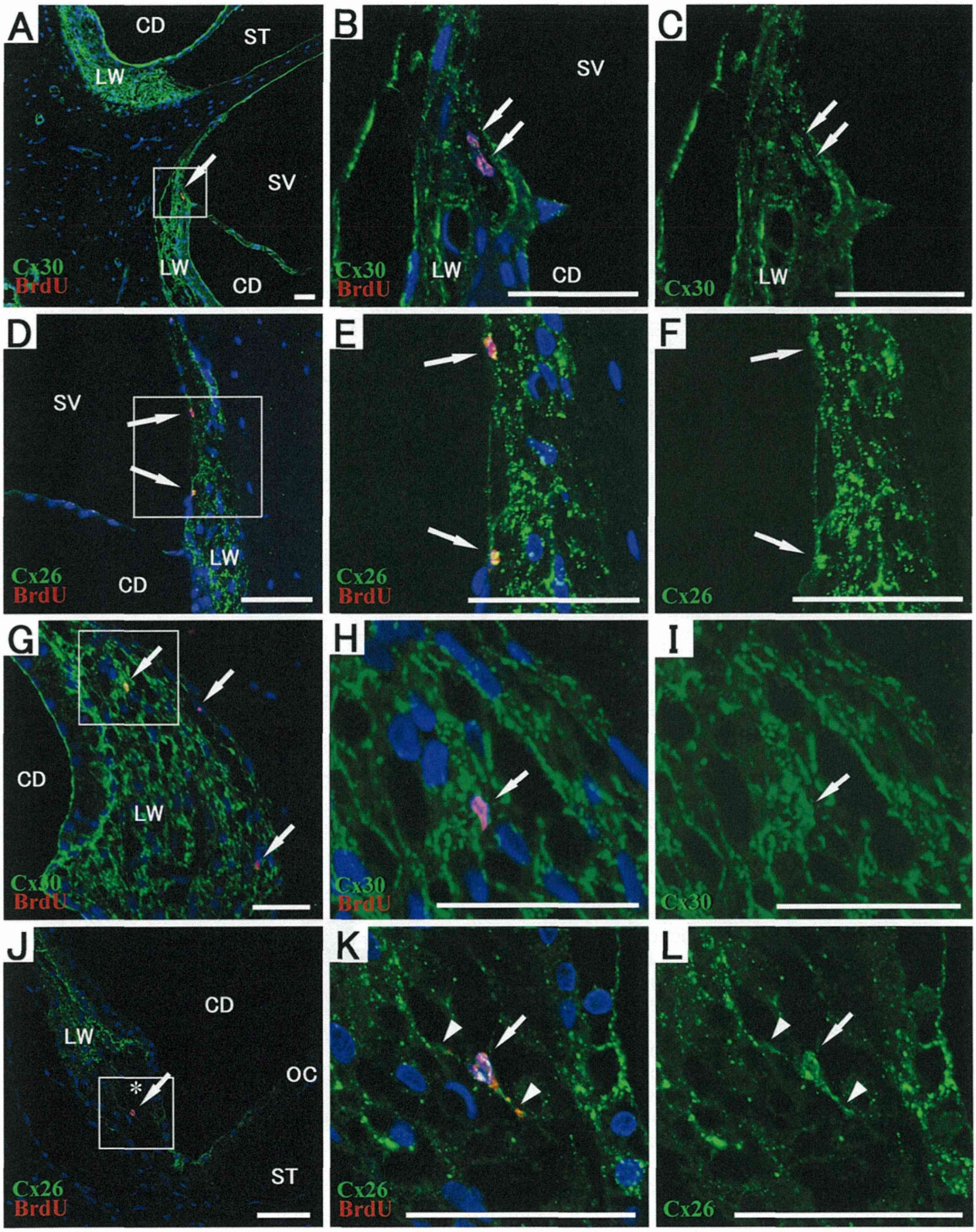

Figure 5. Expression of gap junction proteins Cx30 and Cx26 in transplanted MSCs. MSCs prelabeled with BrdU (red) are shown in the apical part (**A–F**) and middle part (**G–L**) of the lateral wall. Middle and right columns show high-magnification images of the squared area of the panels in the left column. In the right column, only Cx30 or Cx26 expression (green) is shown. **A–C:** In the apical part, weak expression of Cx30 was frequently detected in the BrdU-positive cells (**arrows**) as well as in neighboring fibrocytes. **D–F:** Cx26 expression was also observed in BrdU-positive cells in this area (**arrows**), but spots of immunostaining at cell attachment sites with neighboring fibrocytes were not visible. **G–I:** In the middle part of the lateral wall, strong expression of Cx30 was detected in the transplanted MSCs (**arrows**) as well as in neighboring fibrocytes. In this area, expression of Cx26 was observed in the MSCs even in the severely injured area (**J–L**, **arrow**). These MSCs appeared to have formed new gap junction connections (**arrowheads**) with neighboring fibrocytes. Nuclei were stained with 4,6-diamidino-2-phenylindole (blue). SV, scala vestibuli; CD, cochlear duct; ST, scala tympani; LW, lateral wall; OC, organ of Corti. Scale bars = 50 μm.

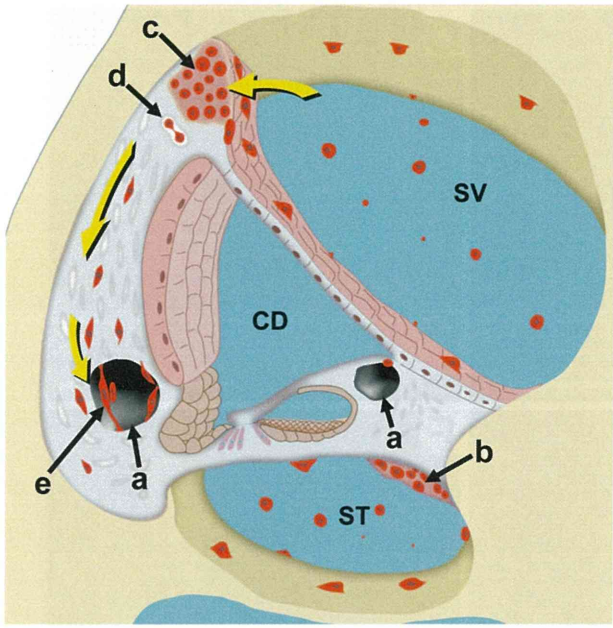

Figure 6. A summary of the histological observations shown in Figures 2, 4, and 5 and our hypothesis for the movements of the transplanted MSCs. The transplanted MSCs are represented in red. **Yellow arrows** indicate the hypothetical route of MSC migration to the injured area (**a**). Some MSCs (**b**) formed a cell mass around the scala tympani. A number of MSCs (**c**) successfully invaded the lateral wall. The invading MSCs (**d**) proliferated in the lateral wall. The MSCs that reached the injured area (**e**) continued to proliferate and repaired the disconnected gap junction network. SV, scala vestibuli; CD, cochlear duct; ST, scala tympani.

lated with a severe foci of apoptotic cochlear fibrocytes in the lateral wall and spiral limbus, both of which are indispensable to the potassium recycling system of the cochlea. The active uptake and passive conductance of K^+ by Na,K-ATPase and the gap junctions, respectively, maintain the endocochlear potential of the endolymph to generate acoustic depolarization of cochlear hair cells through a mechanically gated cation channel.[28] Furthermore, Na,K-ATPase is highly expressed in type II fibrocytes located lateral to the spiral prominence epithelium and suprastrial region.[29] In the case of a cochlear energy shortage induced by 3NP, it is assumed that the active uptake of K^+ by Na,K-ATPase would not continue but the passive conductance of K^+ via gap junctions would be maintained, resulting in an overall decrease of cytosolic $[K^+]$ in a part of the lateral wall and spiral limbus. Because potassium deprivation is a well-known cause of apoptosis,[30] the apoptosis of the cochlear fibrocytes we observed is likely because of low cytosolic $[K^+]$.

In the BrdU incorporation assay, active regeneration of the fibrocytes was observed near the apoptotic area in the lateral wall, suggesting that reconstruction of the potassium recycling route by cellular regeneration led to normalization of endocochlear potential and hearing recovery. Thus, regeneration of cochlear fibrocytes may be an essential process for hearing recovery after acute cochlear energy shortage (such as sudden hearing loss attributable to inner ear ischemia). These spontaneously regenerated cells are thought to be mainly generated by the mitosis of cochlear fibrocytes around the injured area.

However, the recent report suggests that bone marrow cells also have the capacity to migrate into the lateral wall and differentiate into the cochlear fibrocytes.[22]

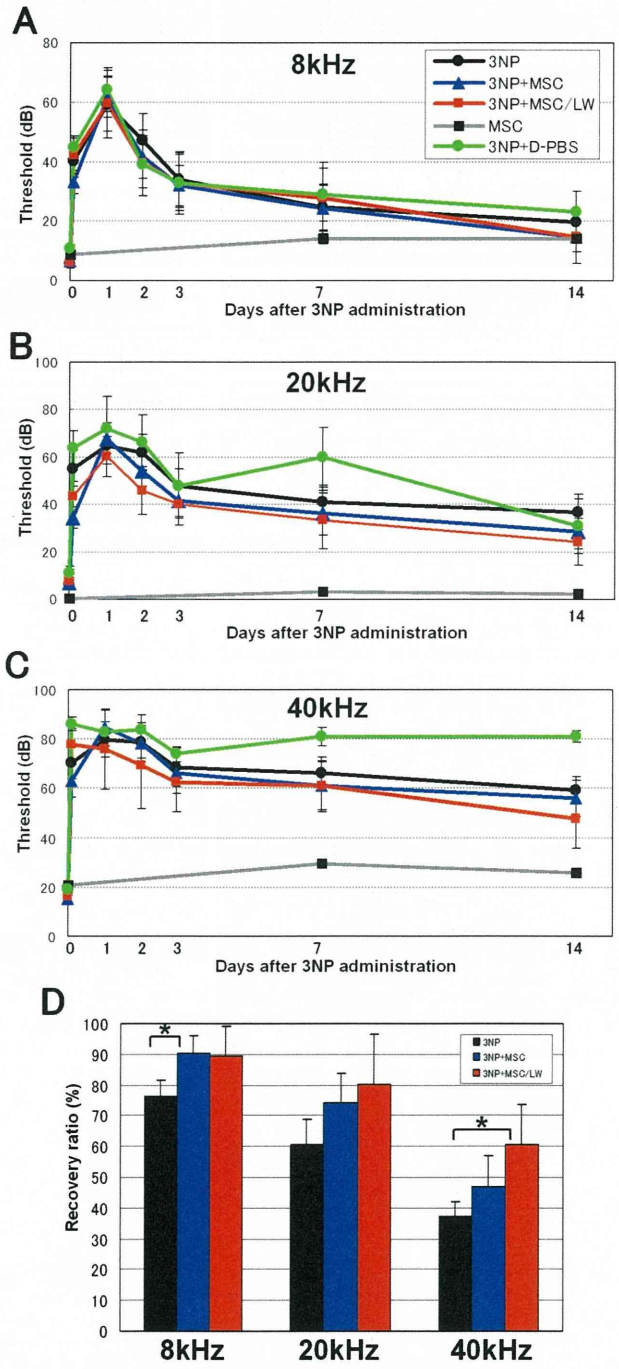

Figure 7. Hearing recovery after MSC transplantation. Thresholds of ABR for 8 (**A**), 20 (**B**), and 40 kHz (**C**) were recorded at 2 hours, 1 day, 2 days, 3 days, 7 days, and 14 days after 3NP administration. **A–C:** ABR thresholds are shown for rats with 3NP administration only (3NP, **black circle**), rats with MSC transplantation at 3 days after 3NP administration (3NP + MSC, **blue triangle**), rats with MSC transplantation at 3 days after 3NP administration and after histological confirmation of MSC invasion into the lateral wall (3NP + MSC/LW, **red square**), rats with MSC transplantation without 3NP administration (MSC, **black square**), and rats with vehicle injection (3NP + D-PBS, **green circle**). **D:** Hearing recovery ratios were calculated from ABR recovery thresholds at 2 weeks. The recovery ratios of 3NP + MSC rats (blue) and 3NP + MSC/LW rats (red) were higher than 3NP rats (black) at all frequencies. $^*P < 0.05$.

Transplantation of MSCs Accelerated Hearing Recovery

The 3NP-treated rats showed complete hearing recovery at low frequencies; however, there remained a residual hearing loss at higher frequencies. Considering that the cochlear fibrocytes that were injured in this model are mesenchymal in origin, we transplanted rat MSCs into the cochlea to attempt to rescue the residual hearing loss. We used MSCs, which we previously established and demonstrated their potential as MSCs, and we further confirmed the surface antigen expression of the cells used for transplantation in flow cytometry, which showed similar expression pattern to human and murine MSCs. This suggests that the cells maintained the capacity as rat MSCs at the moment of transplantation. Because there is no barrier in the inner ear perilymph between the cochlear and vestibular compartments, cells delivered from the lateral semicircular canal by perilymphatic perfusion are considered to have reached the cochlea. Within the perilymph of the cochlea, these cells presumably spread through the scala vestibuli toward the apical turn of the cochlea, and then, after passing through the helicotrema where the scala vestibuli communicates with the scala tympani, kept moving through the scala tympani toward the basal turn. There is no other way in which MSCs can spread within the cochlear perilymph.

Our study clearly demonstrates that rat MSCs were successfully transplanted into the inner ear of 3NP-treated rats by perilymphatic perfusion from the lateral semicircular canal. A number of MSCs were detected on the surface of the ampullary crest facing the perilymph and some of them were detected within the tissue of the ampullary crest, indicating that MSCs survived at least for 11 days after the perfusion and had maintained their ability to invade and migrate into the inner ear tissue. A small number of MSCs appeared to have been rejected by the host tissue in the ampullary crest. This may be attributable to differences between the F344 and Sprague-Dawley rat strains used. In the cochlea, a number of MSCs formed cell masses on the surface of the scala timpani, where the majority of the surrounding tissue is bone tissue, suggesting that these MSCs did not invade the cochlear tissue. In the scala vestibuli, a small number of MSCs were also found attached to the surface of the bone and the Reissner membrane. However, in the apical part of the lateral wall, a number of MSCs were observed within the tissue, suggesting that MSCs had successfully invaded the lateral wall from the perilymph. This area may be an optimum site for MSC invasion.

Furthermore, some of MSCs within the tissue appeared to be undergoing mitosis and forming cell clusters, suggesting that MSCs can proliferate in the injured lateral wall to substitute for the fibrocytes lost through injury. It is likely that the MSCs that invaded the tissue from the apical part of the lateral wall migrated to the injured area in the middle part of the lateral wall. Invasion of MSCs into the lateral wall was observed in half of the rats that had 3NP treatment and MSC transplantation but in only one of seven rats that underwent only MSC transplantation, demonstrating that rats with injury in the lateral wall had a higher rate of MSC invasion than those without injury. The approximate number of BrdU-positive cells in the whole lateral wall with 3NP treatment and MSC transplantation estimated from the immunostained cross sections is 3000 to 5000 cells in single cochlea, and it is 3 to 5% of total cells transplanted by the cell perfusion. It is known that transplanted stem cells are recruited to injury sites by chemokines.[31] Recently, we performed DNA microarray analysis of the cochlear lateral wall RNAs in 3NP-treated rats and found a significant increase in the expression of the small inducible cytokine A2 gene encoding monocyte chemoattractant protein 1 (MCP1, data not shown), which has been reported as a chemokine that induces migration of neural stem cells.[32] This may suggests that the MSC migration to the injured area of the lateral wall in this study may also be induced by chemokines because most MSCs were observed in the lateral wall in basal turn, which had a prominent damage, but not in the apical turn.

One of the most important roles of the cochlear fibrocytes is potassium ion transport for the potassium recycling system within the cochlea, and the gap junction network is essential for ion movement in this system. Thus, we analyzed the expression and distribution of the gap junction proteins Cx30 and Cx26 after MSC transplantation and found that some MSCs within the tissue in the middle part of the lateral wall showed a distribution of Cx30 and Cx26 similar to that of normal cochlear fibrocytes in the same part of the lateral wall. We also observed that MSCs that had invaded the injured area had processes that protruded toward neighboring fibrocytes with condensed Cx26 expression at the tips of the processes, suggesting that these cells invaded the injured area and reconstructed a new gap junction network with the remaining fibrocytes in the area. Moreover, these cells occasionally showed a morphology of dividing cells, suggesting that invading MSCs in the injured area could still proliferate. On the other hand, MSCs observed in the apical part of the lateral wall, which probably represented newly invading MSCs, did not show gap junction connections with their neighboring fibrocytes. The MSCs forming a cell cluster in this region had a round shape without attachments to other fibrocytes, suggesting that these MSCs may still have had stem cell potential and migratory abilities and did not contribute to ion transport. Nuclear expression of connexins in MSCs may indicate that such MSCs were not completely differentiated as cochlear fibrocytes. Nuclear expression of other connexins has been reported in the other types of cells.[33–35] Although functional significance of nuclear expression of connexins is primarily unknown, a recent study reported that nuclear expression of connexins might exert effects on gene expression and cell growth.[36] In this study, invasion of the injured lateral wall by MSCs was histologically confirmed in only 50% of the treated rats, but the rate of MSC invasion of the target area could be improved by using isogenic or autologous transplantation. Otherwise, the addition of appropriate growth factors or continuous transplantation of MSCs may also improve the rates of MSC invasion.

A recent study reported that BrdU could be transferred from prelabeled grafted bone marrow cells to host neuronal precursors and glia.[37] Because BrdU was used to label MSCs in this study, the origin of BrdU-positive cells detected in the cochlea after MSC transplantation needs to be addressed. In the 3NP-treated rats without MSC transplantation, regenerating fibrocytes were confined around the area of apoptosis, which was clearly demarcated in the center of cochlear lateral wall. On the other hand, in the 3NP-treated rats with MSC transplantation, BrdU-positive cells were dispersed from the apical part to the central part within the lateral wall. Furthermore, morphology of BrdU-positive cells was different from neighboring fibrocytes of host tissue in both the apical part and the central part (especially in apical part as shown in Figure 4F). These findings indicate that most of BrdU-positive cells detected within the lateral wall were MSC-derived cells. However, there remains a possibility that a part of BrdU-positive cells around the area of apoptosis may be regenerating fibrocytes taking up BrdU from grafted MSCs. This question will be answered by future studies using MSCs with stable expression of green fluorescent protein by transfection of lentivirus-green fluorescent protein as donor cells.

In this study, we demonstrated that MSC transplantation into cochlea damaged by an acute energy shortage caused a significant improvement in hearing. In particular, the recovery ratio of the ABR threshold at 40 kHz was ~23% higher in the 3NP-treated rats that showed invasion of the lateral wall by MSCs than in 3NP-treated rats without MSC transplantation. This hearing recovery is thought to be caused by the supplement of fibrocytes differentiated from transplanted MSCs in the lateral wall in the basal and middle turn of cochlea. There may be an alternative possibility that the invaded MSCs induced the fibrocellular regeneration in the injured area in lateral wall. In the cochlea, the apical turn receives low-frequency sound and basal turn receives high-frequency sound such as ultrasound at least 80 kHz in rat. The cochlear region, which receives 40 kHz sound, in rat is thought to be around middle to basal turn. In this study, a number of BrdU-positive cells were found in the basal turn including the hook region, as shown in Figure 4, and this might result in the higher recovery ratio shown in 40 kHz. Without therapeutic intervention, the ABR thresholds for 40 kHz showed no improvement between 14 and 42 days after 3NP administration, suggesting that hearing loss for high-frequency sound was permanent. Thus, the MSC transplantation proved to be an effective therapy for this permanent hearing loss.

Because the vehicle injection instead of MSC suspension aggravated ABR thresholds at high frequencies, accelerated hearing recovery by MSC transplantation was considered to be induced by the effect of transplanted MSCs but not by the effect of surgical manipulation. We assume that the aggravated ABR thresholds at high frequencies may be caused by washout of secreted growth factors within the perilymph. The difference in the effects on ABR thresholds at high and low frequencies may be explained by the distinct distances from the semicircular canals where perilymphatic perfusion was conducted. It is likely that the washout effect of perilymphatic perfusion was bigger in the high frequency area than in the low-frequency area because the high-frequency area is located closer to the semicircular canals.

Recently, stem cell transplantation directly into the inner ear has been reported in several animal experiments[38,39]; however, data demonstrating successful improvement of hearing after these transplantations have not been reported. In addition, few reports have shown any convincing evidence that transplanted cells have invaded the injured region and repaired the structure and function. The failure to improve hearing in the previous studies may be related to the surgical methods used to deliver stem cells into the cochlea. In this study, we transplanted MSCs by cell perfusion from the lateral semicircular canal with drainage to the posterior semicircular canal to minimize the surgical effects on the cochlea. This method is similar to a recently reported technique that demonstrated the integrity of hearing function after delivery of stem cells to the inner ear[40] and confirmed that the operation produced no significant hearing defects in normal control rats.

Bone marrow MSCs have greater advantages for clinical use in human patients than other multipotential stem cells, such as embryonic stem cells because MSCs can be collected from the patient's own bone marrow for an autologous transplantation with little physical risk, no rejection risk, and few ethical problems. In the present transplantation, many MSCs were confirmed to have invaded the lateral wall and to have contributed to recovery of hearing loss despite transplantation between different rat strains. Therefore, we expect that autologous transplantation of bone marrow MSCs would be even more effective in treating hearing loss caused by injuries to the cochlear fibrocytes. In addition, significant improvement of hearing by MSC transplantation between different rat strains indicates a possibility of allogenic transplant. Even temporary effects by allogenic transplant may cause difference in the final outcome of hearing recovery by promoting regeneration or viability of host fibrocytes during acute period of injury.

This is the first report demonstrating that MSC transplantation improves incomplete hearing recovery with evidence that transplanted MSCs actually invaded the injured area and contributed to the structural reorganization of the injured cochlea. Cell therapy targeting regeneration of the cochlear fibrocytes may therefore be a powerful strategy to cure sensorineural hearing loss that cannot be reversed by current therapies.

Acknowledgments

We thank Drs. Yasuhiro Yoshikawa, Juichi Ito, Takeshi Iwata, and Yoshiyuki Ishii for their valuable help in the experiments.

References

1. Wangemann P: K^+ cycling and the endocochlear potential. Hear Res 2002, 165:1–9

2. Weber PC, Cunningham III CD, Schulte BA: Potassium recycling pathways in the human cochlea. Laryngoscope 2001, 111:1156–1165
3. Delprat B, Ruel J, Guitton MJ, Hamard G, Lenoir M, Pujol R, Puel J-L, Brabet P, Hamel CP: Deafness and cochlear fibrocyte alterations in mice deficient for the inner ear protein otospiralin. Mol Cell Biol 2005, 25:847–853
4. Kikuchi T, Kimura RS, Paul DL, Adams JC: Gap junctions in the rat cochlea: immunohistochemical and ultrastructural analysis. Anat Embryol (Berl) 1995, 191:101–118
5. Spicer SS, Schulte BA: The fine structure of spiral ligament cells relates to ion return to the stria and varies with place-frequency. Hear Res 1996, 100:80–100
6. Minowa O, Ikeda K, Sugitani Y, Oshima T, Nakai S, Katori Y, Suzuki M, Furukawa M, Kawase T, Zheng Y, Ogura M, Asada Y, Watanabe K, Yamanaka H, Gotoh S, Nishi-Takeshima M, Sugimoto T, Kikuchi T, Takasaka T, Noda T: Altered cochlear fibrocytes in a mouse model of DFN3 nonsyndromic deafness. Science 1999, 285:1408–1411
7. Xia AP, Kikuchi T, Minowa O, Katori Y, Oshima T, Noda T, Ikeda K: Late-onset hearing loss in a mouse model of DFN3 non-syndromic deafness: morphologic and immunohistochemical analyses. Hear Res 2002, 166:150–158
8. Spicer SS, Schulte BA: Spiral ligament pathology in quiet-aged gerbils. Hear Res 2002, 172:172–185
9. Hequembourg S, Liberman MC: Spiral ligament pathology: a major aspect of age-related cochlear degeneration in C57BL/6 mice. J Assoc Res Otolaryngol 2001, 2:118–129
10. Wu T, Marcus DC: Age-related changes in cochlear endolymphatic potassium and potential in CD-1 and CBA/CaJ mice. J Assoc Res Otolaryngol 2003, 4:353–362
11. Kelsell DP, Dunlop J, Stevens HP, Lench NJ, Liang JN, Parry G, Mueller RF, Leigh IM: Connexin 26 mutations in hereditary nonsyndromic sensorineural deafness. Nature 1997, 387:80–83
12. del Castillo I, Villamar M, Moreno-Pelayo MA, del Castillo FJ, Alvarez A, Telleria D, Menendez I, Moreno F: A deletion involving the connexin 30 gene in nonsyndromic hearing impairment. N Engl J Med 2002, 346:243–249
13. Hoya N, Okamoto Y, Kamiya K, Fujii M, Matsunaga T: A novel animal model of acute cochlear mitochondrial dysfunction. Neuroreport 2004, 15:1597–1600
14. Okamoto Y, Hoya N, Kamiya K, Fujii M, Ogawa K, Matsunaga T: Permanent threshold shift caused by acute cochlear mitochondrial dysfunction is primarily mediated by degeneration of the lateral wall of the cochlea. Audiol Neurootol 2005, 10:220–233
15. Alston TA, Mela L, Bright HJ: 3-Nitropropionate, the toxic substance of Indigofera, is a suicide inactivator of succinate dehydrogenase. Proc Natl Acad Sci USA 1977, 74:3767–3771
16. Coles CJ, Edmondson DE, Singer TP: Inactivation of succinate dehydrogenase by 3-nitropropionate. J Biol Chem 1979, 254:5161–5167
17. Brouillet E, Hantraye P, Ferrante RJ, Dolan R, Leroy-Willig A, Kowall NW, Beal MF: Chronic mitochondrial energy impairment produces selective striatal degeneration and abnormal choreiform movements in primates. Proc Natl Acad Sci USA 1995, 92:7105–7109
18. Hamilton BF, Gould DH: Nature and distribution of brain lesions in rats intoxicated with 3-nitropropionic acid: a type of hypoxic (energy deficient) brain damage. Acta Neuropathol (Berl) 1987, 72:286–297
19. Pittenger MF, Mackay AM, Beck SC, Jaiswal RK, Douglas R, Mosca JD, Moorman MA, Simonetti DW, Craig S, Marshak DR: Multilineage potential of adult human mesenchymal stem cells. Science 1999, 284:143–147
20. Liechty KW, MacKenzie TC, Shaaban AF, Radu A, Moseley AM, Deans R, Marshak DR, Flake AW: Human mesenchymal stem cells engraft and demonstrate site-specific differentiation after in utero transplantation in sheep. Nat Med 2000, 6:1282–1286
21. Jiang Y, Jahagirdar BN, Reinhardt RL, Schwartz RE, Keene CD, Ortiz-Gonzalez XR, Reyes M, Lenvik T, Lund T, Blackstad M, Du J, Aldrich S, Lisberg A, Low WC, Largaespada DA, Verfaillie CM: Pluripotency of mesenchymal stem cells derived from adult marrow. Nature 2002, 418:41–49
22. Lang H, Ebihara Y, Schmiedt RA, Minamiguchi H, Zhou D, Smythe N, Liu L, Ogawa M, Schulte BA: Contribution of bone marrow hematopoietic stem cells to adult mouse inner ear: mesenchymal cells and fibrocytes. J Comp Neurol 2006, 496:187–201
23. Kamiya K, Takahashi K, Kitamura K, Momoi T, Yoshikawa Y: Mitosis and apoptosis in postnatal auditory system of the C3H/He strain. Brain Res 2001, 901:296–302
24. Satoh H, Kishi K, Tanaka T, Kubota Y, Nakajima T, Akasaka Y, Ishii T: Transplanted mesenchymal stem cells are effective for skin regeneration in acute cutaneous wounds. Cell Transplant 2004, 13:405–412
25. Kicic A, Shen WY, Wilson AS, Constable IJ, Robertson T, Rakoczy PE: Differentiation of marrow stromal cells into photoreceptors in the rat eye. J Neurosci 2003, 23:7742–7749
26. Colter DC, Sekiya I, Prockop DJ: Identification of a subpopulation of rapidly self-renewing and multipotential adult stem cells in colonies of human marrow stromal cells. Proc Natl Acad Sci USA 2001, 98:7841–7845
27. Peister A, Mellad JA, Larson BL, Hall BM, Gibson LF, Prockop DJ: Adult stem cells from bone marrow (MSCs) isolated from different strains of inbred mice vary in surface epitopes, rates of proliferation, and differentiation potential. Blood 2004, 103:1662–1668
28. Corey DP, Hudspeth AJ: Ionic basis of the receptor potential in a vertebrate hair cell. Nature 1979, 281:675–677
29. Suko T, Ichimiya I, Yoshida K, Suzuki M, Mogi G: Classification and culture of spiral ligament fibrocytes from mice. Hear Res 2000, 140:137–144
30. Schulz JB, Weller M, Klockgether T: Potassium deprivation-induced apoptosis of cerebellar granule neurons: a sequential requirement for new mRNA and protein synthesis, ICE-like protease activity, and reactive oxygen species. J Neurosci 1996, 16:4696–4706
31. Imitola J, Raddassi K, Park KI, Mueller FJ, Nieto M, Teng YD, Frenkel D, Li J, Sidman RL, Walsh CA, Snyder EY, Khoury SJ: Directed migration of neural stem cells to sites of CNS injury by the stromal cell-derived factor 1alpha/CXC chemokine receptor 4 pathway. Proc Natl Acad Sci USA 2004, 101:18117–18122
32. Widera D, Holtkamp W, Entschladen F, Niggemann B, Zanker K, Kaltschmidt B, Kaltschmidt C: MCP-1 induces migration of adult neural stem cells. Eur J Cell Biol 2004, 83:381–387
33. Eisner I, Colombo JA: Detection of a novel pattern of connexin 43 immunoreactivity responsive to dehydration in rat hypothalamic magnocellular nuclei. Exp Neurol 2002, 177:321–325
34. de Feijter AW, Matesic DF, Ruch RJ, Guan X, Chang CC, Trosko JE: Localization and function of the connexin 43 gap-junction protein in normal and various oncogene-expressing rat liver epithelial cells. Mol Carcinog 1996, 16:203–212
35. Honma S, De S, Li D, Shuler CF, Turman Jr JE: Developmental regulation of connexins 26, 32, 36, and 43 in trigeminal neurons. Synapse 2004, 52:258–271
36. Dang X, Doble BW, Kardami E: The carboxy-tail of connexin-43 localizes to the nucleus and inhibits cell growth. Mol Cell Biochem 2003, 242:35–38
37. Burns TC, Ortiz-Gonzalez XR, Gutierrez-Perez M, Keene CD, Sharda R, Demorest ZL, Jiang Y, Nelson-Holte M, Soriano M, Nakagawa Y, Luquin MR, Garcia-Verdugo JM, Prosper F, Low WC, Verfaillie CM: Thymidine analogs are transferred from prelabeled donor to host cells in the central nervous system after transplantation: a word of caution. Stem Cells 2006, 24:1121–1127
38. Naito Y, Nakamura T, Nakagawa T, Iguchi F, Endo T, Fujino K, Kim TS, Hiratsuka Y, Tamura T, Kanemaru S, Shimizu Y, Ito J: Transplantation of bone marrow stromal cells into the cochlea of chinchillas. Neuroreport 2004, 15:1–4
39. Hu Z, Wei D, Johansson CB, Holmstrom N, Duan M, Frisen J, Ulfendahl M: Survival and neural differentiation of adult neural stem cells transplanted into the mature inner ear. Exp Cell Res 2005, 302:40–47
40. Iguchi F, Nakagawa T, Tateya I, Endo T, Kim TS, Dong Y, Kita T, Kojima K, Naito Y, Omori K, Ito J: Surgical techniques for cell transplantation into the mouse cochlea. Acta Otolaryngol Suppl 2004, (551):43–47